

THE DIRECT DETERMINATION OF NICOTINE
BY CIRCULAR DICHROISM
SPECTROPOLARIMETRY

By

WILLIAM MARC ATKINSON

Bachelor of Science

Ouachita Baptist University

Arkadelphia, Arkansas

1980

Submitted to the Faculty of the
Graduate College of the
Oklahoma State University
in partial fulfillment of
the requirements for
the Degree of
MASTER OF SCIENCE
May, 1983

Thesis
1983
A878d
copy 2

Name: William Marc Atkinson Date of Degree: May, 1983

Institution: Oklahoma State University

Location: Stillwater, Oklahoma

Title of Study: THE DIRECT DETERMINATION OF NICOTINE BY
CIRCULAR DICHROISM SPECTROPOLARIMETRY



Pages in Study: 66

Candidate for Degree of Master
of Science

Major Field: Chemistry

Scope and Method of Study: Circular Dichroism (CD), a non-traditional analytical technique, is evaluated for the analysis of nicotine and its major metabolite cotinine. A comparison of the CD and uv-visible methods for the analysis of nicotine in tobacco samples exemplifies many of the advantages the CD method has over other methods of analysis. The CD spectra of nicotine and cotinine are characterized and methods for the subsequent quantitative analysis are outlined. The binding constant for a nicotine- β -cyclodextrin complex is determined and efforts to analyze a cotinine/nicotine binary mixture are described.

Findings and Conclusions: Circular dichroism is found to be a potentially powerful analytical technique for the analysis of nicotine. The interferences that seemingly cripple many other optical methods did not present any problems with the CD technique. Although the binding between nicotine and β -cyclodextrin manifested only a small change in the observed spectrum, the calculation of a binding constant was possible. The cotinine/nicotine mixture analysis was unsuccessful due to the visual similarities in the spectra of the standards and the large difference in the molar ellipticities of the two species.

ADVISER'S APPROVAL

W. C. Purdie

THE DIRECT DETERMINATION OF NICOTINE
BY CIRCULAR DICHROISM
SPECTROPOLARIMETRY

Thesis Approved:

W. C. Purdie

Thesis Adviser

Horacio A. Mottola

Sunda B. McGowan

Norman N. Durham

Dean of the Graduate College

PREFACE

The objective of this study was to develop a method for the direct determination of nicotine and its major metabolite, cotinine, using circular dichroism spectropolarimetry.

I wish to express my sincere gratitude to Dr. Neil Purdie for his invaluable guidance and unending support throughout this study. His aid in the preparation of the manuscript was extremely helpful. I also wish to thank the members of my faculty committee, Drs. H. A. Mottola and L. B. McGown, for their help and encouragement throughout my stay at this university. Gratitude is also extended to my fellow graduate students and the complete faculty and staff of the Chemistry department for their unfailing encouragement.

I would also like to express my gratitude to my parents, Mr. and Mrs. W. K. Atkinson and my brothers, Chuck and Drew, for their patience and loving support.

This study was supported by the National Science Foundation under their grant number NSF CHE 7909388.

TABLE OF CONTENTS

Chapter	Page
I. INTRODUCTION	1
II. BACKGROUND AND THEORY	6
III. EXPERIMENTAL	23
Instrumental	23
Chemicals	26
Experimenetal Procedures	26
IV. EXPERIMENTAL RESULTS	30
The Circular Dichroic Spectra of Nicotine .	31
Linear Dynamic Range for Nicotine	31
Determination of Nicotine in Smokeless Tobaccos	38
Calculation of β - Cyclodextrin - Nicotine Constant (K_{bind})	46
Determination of Cotinine	56
V. CONCLUSION	62
A SELECTED BIBLIOGRAPHY	64
APPENDIX	66

LIST OF TABLES

Table	Page
I. Properties of Nicotine	3
II. Birefringence Polarizers and Invention Dates .	10
III. Rainin Pipetman Specifications**	27
IV. CD Spectral Characteristic of Nicotine	33
V. Kiaser's Limit of Detection For Isopropanioc Nicotine Solutions at 236, 255, and 261 Nanometers	39
VI. Percent Nicotine By Weight in SKOAL Versus Extraction Time Data	46
VII. Smokeless Tobacco Nicotine Analysis Results* .	48
VIII. pH Change in an Unbuffered Aqueous Solution Corresponding to Total Nicotine Concen- tration Changes*	49
IX. Spectral Characteristics of 8.2 pH Buffered Nicotine Solutions	52
X. Properties of Cotinine	58
XI. Circular Dichroic Characteristics of Cotinine in pH 8.2	58

LIST OF FIGURES

Figure	Page
1. The Oxidation of Nicotine Into Cotinine	2
2. Wave Motion Propagated in the X Direction by Transverse Vibration. λ is the Wavelength. The Vertical Lines Represent the Electric Field Vector at a Given Instant as the Light Wave Progresses Along the X Axis	7
3. Schematic Representation of Unpolarized and Linearly Polarized Light. (a) Cross-section of a Beam of Light Traveling Toward the Viewer. The Light Waves Can Vibrate in Any Direction that is Perpendicular to the Line of Travel. (b) A Beam of Linearly Polarized Light Has Vibrations Only in the Plane of Polarization .	8
4. The Rochon Birefringence Prism	11
5. End View of the Electric Field Vector E as the Result of Two Rotating Vectors E_R and E_L	13
6. End View of Electric Field Vectors on Passage of Linearly Polarized Light Through an Optically Active Material. α is the Observed Rotation .	15
7. End View of Electric Field Vectors on Passage of Linearly Polarized Light Through an Optically Active Material. The Wavelength of Light is Near an Absorption Band	17
8. Ring Structure of β -cyclodextrin	22
9. Schematic of an Inclusion Complex	22
10. Optical System of the JASCO J-500 Circular Dichroism Spectropolarimeter. Source: JASCO .	24
11. The Isopropanoic Circular Dichroic Spectra of Nicotine	32
12. Observed Ellipticity Versus Nicotine Concentration Calibration Curve and Linear Regression Analysis Statistics. Solvent: Isopropanol . .	34

Figure	Page
13. Absolute Value of Observed Ellipticity Versus Nicotine Concentration Calibration Curve and Linear Regression Statistics. Solvent: Isopropanol	35
14. Absolute Value of Observed Ellipticity Versus Nicotine Concentration Calibration Curve and Linear Regression Statistics. Solvent: Isopropanol	36
15. The UV Spectra of a) Pure Nicotine and b) The Extract From A Smokeless Tobacco Sample	41
16. The CD Spectra of a) Pure Nicotine and b) The Extract From A Smokeless Tobacco Sample	42
17. Percent Nicotine by Weight in SKOAL Versus Extraction Time	44
18. α Versus pH Diagram For Nicotine	50
19. Plot of Equation 3.3 for 268 Nanometers With Linear Regression Statistics	54
20. Plot of Equation 3.3 for 261 Nanometers With Linear Regression Statistics	55
21. CD Spectra of Cotinine in 8.2 pH Buffer	59
22. Observed Ellipticity Versus Cotinine Concentra- tion Calibration Curve and Linear Regression Analysis Statistics. Solvent: 8.2 pH Buffer .	60
23. Observed Ellipticity Versus Cotinine Concentra- tion Calibration Curve and Linear Regression Analysis Statistics. Solvent: 8.2 pH Buffer .	61

CHAPTER I

INTRODUCTION

Nicotine, a common alkaloid present in all forms of tobacco, functions as an addictive-like agent in the body. Habitual tobacco users often require a nicotine boost every twenty to thirty minutes throughout the waking hours (1).

Nicotine has been used extensively as an agricultural fumigant, a contact poison for microorganisms, and a stomach poison. The insecticidal use of nicotine per year amounts to over 500 tons in the United States alone (2). Commercial nicotine is entirely a byproduct of the tobacco industry.

Nicotine is described as highly toxic (2) and has been listed as one of the most toxic substances known (3). The lethal dose in man is forty to sixty milligrams per kilogram of body weight (3). Most poisoning cases are due to careless handling when nicotine is employed as a horticultural insecticide (2).

Nicotine is obtained from the leaves of the tobacco plant, *Nicotiana tabacum* (Solanaceae). It is a colorless to pale yellow, volatile, very hygroscopic, oily liquid which gradually turns brown upon exposure to air and/or light. Nicotine is soluble in water, alcohols, ethers, chloroform

and oils (2). Table I contains a list of nicotine properties.

Nicotine is metabolized in man by oxidation at position five of the pyrrolidine ring to yield cotinine (Figure 1). Cotinine can undergo further metabolism by hydroxylation, demethylation or cleavage of the pyrrolidine ring to yield α -(3-pyridyl)- β oxo-N-methylbutyramide (2).

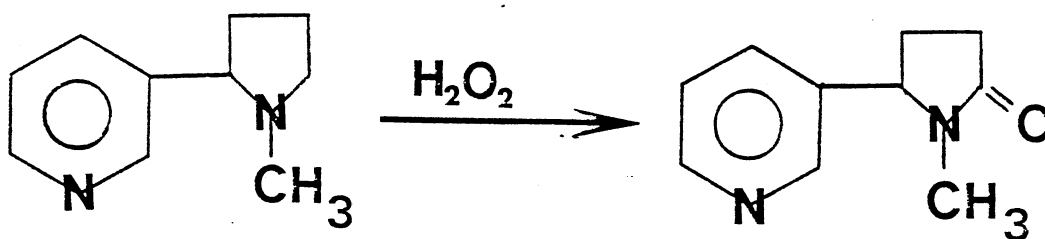


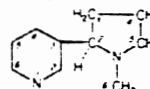
Figure 1. The Oxidation of Nicotine Into Cotinine

Nicotine is readily absorbed through the body organs and membranes such as the lungs and the oral and nasal tissues. The nicotine blood level of smokers is usually less than 0.03%, but the nicotine is readily distributed throughout the body, even into the milk of lactating mothers (4).

Urinary excretion of unchanged nicotine accounts for a small percentage of the administered dose, but increases with urine acidity (5). The major derivative of nicotine found in the urinary tract is cotinine (6).

TABLE I
PROPERTIES OF NICOTINE

Structure:



IUPAC name: S (-) - 3 - (1 - methyl - 2 pyrrolidiny1)
pyridine

Formula:	$C_{10}H_{14}N_2$
Molecular Weight:	162.2 g / mole
Boiling Point:	247° C (754 torr)
Description:	pale yellow, oily liquid
Refractive index (n_D^{20}):	1.5282
Density (d_4^{20}):	1.0097 g / ml
Specific Rotation (α_D^{20}):	-169°
pKa1 @ 15°:	6.16
pKa2 @ 15°:	10.96

Source: Merck Index 9th Edition. E. G. C. Clarke
"Isolation and Identification of Drugs", Vol. 1
The Pharmaceutical Press (1969).

The clinical analysis of nicotine and its metabolites have been reported by numerous authors (7-10). The reported methods of analysis include gas, high-pressure liquid, and thin-layer chromatography, mass spectrometry, uv-visible and infrared spectroscopy. Testa and Jenner have used optical rotatory dispersion (ORD) and circular dichroism spectropolarimetry (CD) along with uv-visible spectroscopy to determine the preferred conformation of nicotine and related chiral alkaloids (11). It cannot, however, be ascertained from a recent literature search, that chiroptical methods have been employed for the quantitative determination of nicotine. Considering the selectivity and sensitivity of the method, this lack of activity comes as somewhat of a surprise. The analytical procedure for such an endeavor has been reported, by my colleagues, in the analysis of numerous illicit drugs, including cocaine, phencyclidine (PCP), and morphine (12).

The stringent requirements that must be met before a species will exhibit a CD spectrum effectively screen out many of the interferences that cause problems with other methods of instrumental analysis. The extract from a nicotine containing sample can be analyzed directly with CD without further separation and/or concentration steps, such as stream distillation, as has been described for other methods (13). The implication, of the removal of these subsequent steps, is that the analysis time per sample can be dramatically reduced. Considering the problems posed on clinical

analysis by modern economics, development of this aspect of the CD method is a lucrative investment of time and effort. The focus of this research has been to develop a circular dichroic method for the quantitative determination of nicotine. Spectral identification and quantification of nicotine and its major metabolite, cotinine, have been characterized.

Earlier work by my co-workers has shown that the CD spectra of some compounds can be altered or induced via complexation with cyclodextrin sugars. They have reported binding constants for such interactions with cocaine and phencyclidine (PCP). The analyte molecule is thought to complex with the cyclodextrin by inclusion into the non-polar cavity of the sugar. Nicotine has shown to exhibit this type of complexation and a binding constant for the nicotine - β -cyclodextrin complex has been calculated.

CHAPTER II

BACKGROUND AND THEORY

Analysis for optically active (chiral) molecules has been a perplexing problem to both organic and analytical chemists. In the early nineteenth century, Biot, a French physicist, discovered that certain naturally occurring organic compounds had the ability to rotate the plane of polarization of linearly polarized light (15). He later found that the rotatory power of these molecules increased as the wavelength of the light decreased (16). The measurement of the degree of rotation versus wavelength became known as Optical Rotatory Dispersion (ORD).

Some thirty years later, Haidenger observed that an amethyst quartz crystal absorbed the left and right handed circularly polarized light components differently (17). This opened the door to a more powerful technique for the analysis of chiral compounds. Upon further development, the measurement of this differential absorption versus wavelength became known as Circular Dichorism Spectropolarimetry (CD).

Although optical rotation was used in some of the earliest structural studies, the fundamental theory is still not thoroughly understood. There have been many attempts to

derive molecular theories and empirical formulae to describe and predict optical activity, but the actual theory has not yet been described.

An understanding of the basic theory must begin with a study of light itself. Light is made up of electric field vectors that oscillate in a sinusoidal wave perpendicular to the direction of propagation (Figure 2).

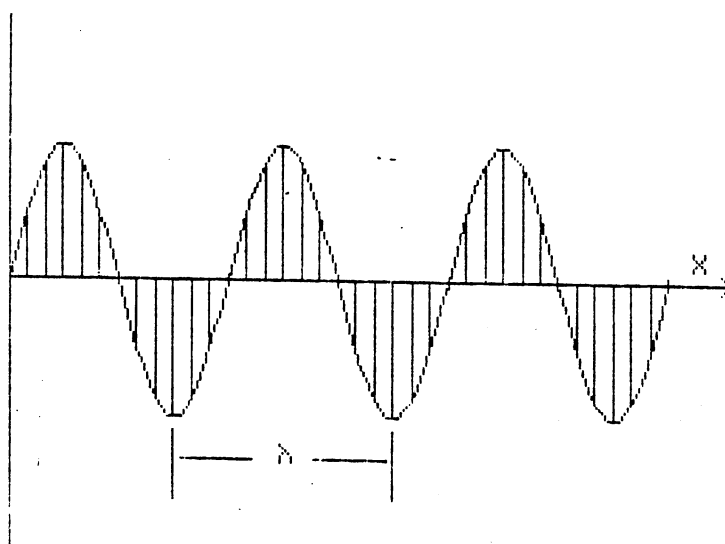


Figure 2. Wave Motion Propagated in the X Direction by Transverse Vibration; λ is the Wavelength. The Vertical Lines Represent the Electric Field Vector at a Given Instant as the Light Wave Progresses Along the X Axis

A magnetic field is associated with this oscillating electric field, but for clarity has been omitted from the diagram.

A beam of light can be thought of as a bundle of waves with vibratory motions distributed over a family of planes, all of which include the axis of propagation. As indicated in Figure 3a, the vibration of the light may be in any direction that is perpendicular to the line of travel. It should be understood that, in normal light, no single direction of vibration predominates over another. In plane polarized light all of the vibrations occur within one plane, the plane of polarization. Linearly polarized light is plane polarized light in which all of the electronic vectors have a parallel line of travel (Figure 3b).

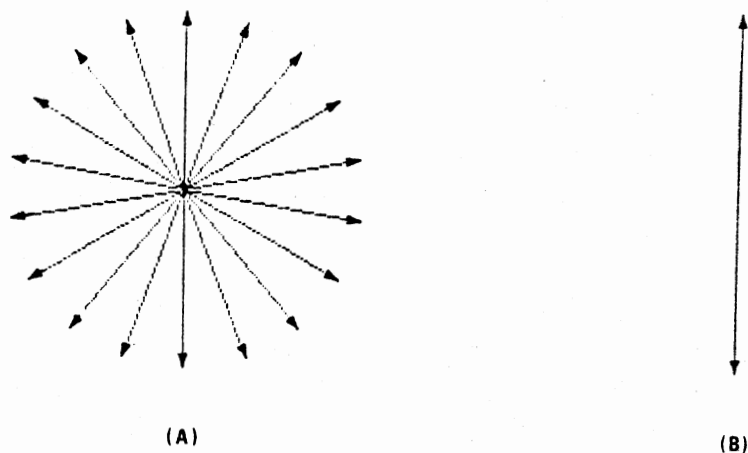


Figure 3. Schematic Representation of Unpolarized and Linearly Polarized Light. (a) Cross-section of a Beam of Light Traveling Toward the Viewer. The Light Waves Can Vibrate in Any Direction that is Perpendicular to the Line of Travel. (b) A Beam of Linearly Polarized Light has Vibrations Only in the Plane of Polarization.

A number of devices have been used for the production of linearly polarized light, such as reflection polarizers, dichroic polarizers, and birefringence polarizers. The practical applications of reflection polarizers are limited because of a number of limitations which include inefficient reflection and the variation of the polarizing angle with wavelength. Some redemptive value can be gained by successive reflections, but efforts to employ this type of polarizer have been abandoned in favor of better alternatives.

Dichroic polarizers are the most widely used for the polarization of visible light. The most common example of this type of polarizer is Polaroid. These polarizers work by selective absorption of the light whose vibrations are not parallel with the Polaroid's optical axis. The use of polaroids in the ultraviolet region is limited by the high absorbance and weak dichroism properties of the material. Because many of the transitions studied via CD are in the ultraviolet regions of the spectra, this type of polarizer is not commonly used with CD spectropolarimeters.

Birefringence polarizers are, by far, the most widely used polarizers in the ultraviolet wavelengths despite the high cost. These polarizers are constructed of uniaxial prisms and operate by resolving the incident beam into two linearly polarized rays; the ordinary and the extraordinary. Table II lists several birefringence polarizers by the inventor's name and invention date. Any of these polarizers

TABLE II
BIREFRINGENCE POLARIZERS AND
INVENTION DATES

Polarizer	Invention Date
Rochon	1811
Wollaston	1820
Nicol	1828
Senarmont	1857
Foucault	1857
Jamin	1869
Glan	1880
Glazebrook	1883
Thompson	1886
Cotton	1931
Glan-Thompson-Taylor	1948

Source: Abu-Shumays and Duffield, Anal. Chem. 38(7), 29A,
(1966).

could be used for CD purposes, but the most commonly used today is the Rochon Type. The Rochon polarizer is made by crossing the optical axes of two prisms cut from a uniaxial crystal (Figure 4). The prisms are placed together in optical contact or separated by a liquid whose index of refraction is very similar to that of the material from which the prisms are made. An incident beam enters the polarizer along an optical axis of one of the crystals and is doubly reflected into two separate beams at the prism interface. The angle by which the two beams are separated is a function of the angles cut into the prisms and the

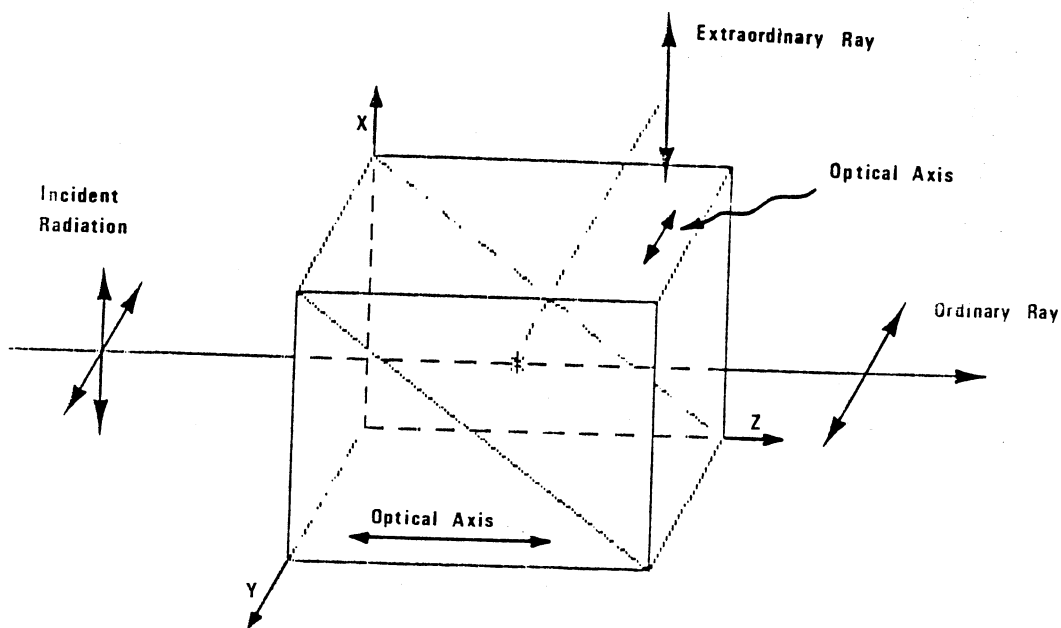


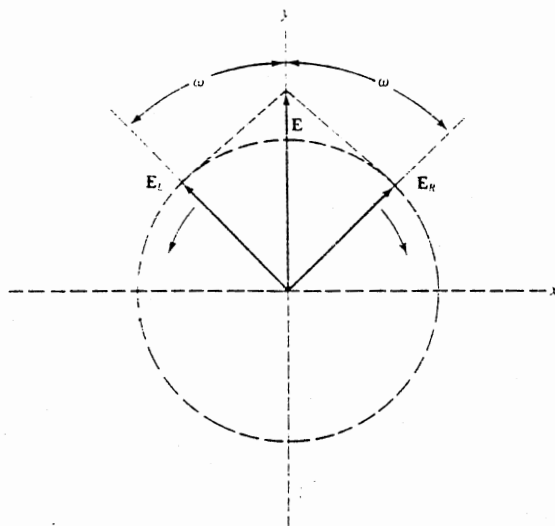
Figure 4. The Rochon Birefringence Prism

birefringence of the crystal material. The ordinary beam is linearly polarized and traverses unperturbed through the polarizer. The extraordinary beam is reflected away and is orthogonally polarized with respect to the ordinary beam.

The crystal material plays an important role in the versatility of the polarizer. The birefringence of the material determines to what degree the ordinary and the extraordinary beams are separated. Another aspect of the crystal material that should be considered is its transparency over the ultraviolet and visible regions. Quartz crystals have been reported to be transparent down to 175 nanometers (18).

Linearly polarized light can be resolved into two circularly polarized components as shown in Figure 5. E is the magnitude of the electric vector oscillating sinusoidally along the axis of propagation and E_R and E_L are the two rotating vectors into which E can be resolved. In other words, linearly polarized light is the vector sum of the two vector components E_R and E_L . These two vector components are identical in magnitude and rotatory frequency, but revolve in opposite angular directions, i.e. clockwise and counter-clockwise. At any moment the vector sum of the two vectors E will lie in the plane of polarization, because the angles ω and ω' are equal functions of time.

When linearly polarized light is passed through a chiral medium, the vectors E_R and E_L will rotate at



Used by permission, E. D. Olsen, "Modern Optical Methods of Analysis", McGraw-Hill, 1975.

Figure 5. End View of the Electric Field Vector E as the Resultant of Two Rotating Vectors, E_R and E_L

different speeds due to the different indices of refraction for the two light components in that medium. As a result $\omega \neq \omega'$. The vector sum E will no longer lie in the original plane of polarization, but will be rotated by an angle α from the y-axis (Figure 6).

Materials or compounds that allow E_R to travel faster than E_L ($\omega > \omega'$) are dextrorotatory and α is assigned a positive (+) sign. Conversely, the medium is labeled levorotatory when the new plane of polarization makes a negative angle with the y-axis ($\omega < \omega'$).

As was stated earlier, the speed or frequency of rotation of the vectors E_R and E_L is a function of the refractive indices of the respective components in a particular medium. Thus, the angle of rotation can be expressed as a function of these indices:

$$\alpha = \frac{\pi}{\lambda (n_L - n_R)} \quad \text{Eq. 2.1}$$

where: α = rotation, rad/unit length

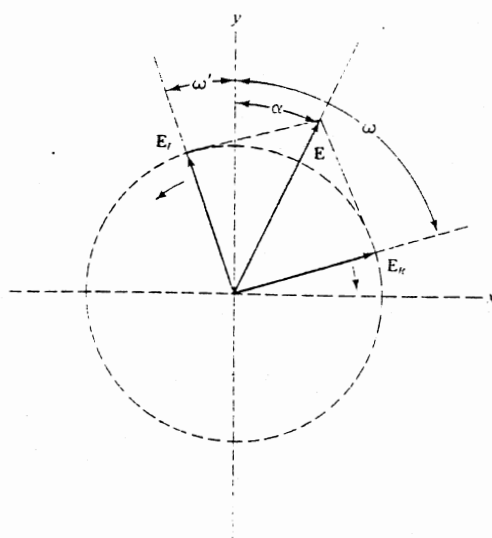
λ = wavelength of incident radiation

n_L = index of refraction for left circularly polarized light

n_R = index of refraction for right circularly polarized light

This rotation α can be converted into a quantity defined as the specific rotation $[\alpha]$, having units of degrees per decimeter per unit concentration:

$$[\alpha] = (\alpha/C)(1800/\pi) \quad \text{Eq. 2.2}$$



Used by permission, E. D. Olsen, "Modern Optical Methods of Analysis", McGraw-Hill, 1975

Figure 6. End View of Electric Field Vectors on Passage of Linearly Polarized Light Through an Optically Active Material. α is the Observed Rotation.

where C is the concentration of the chiral species in grams per milliliter of solution.

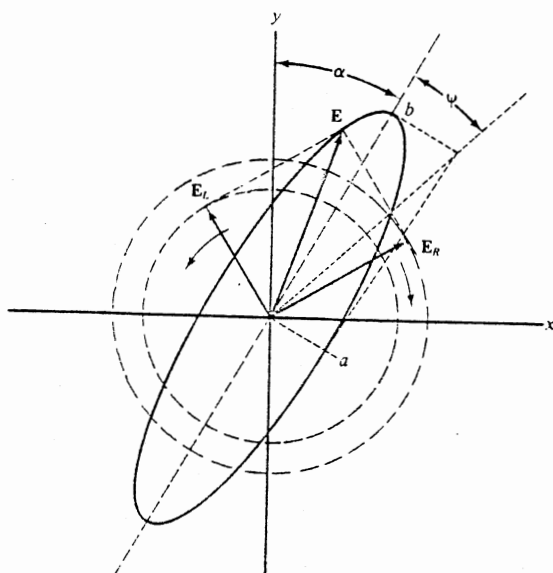
Referring again to Equation 2.1, the value $(n_R - n_L)$ is called the circular birefringence and must have nonzero values for all optically active materials. The variance of the birefringence with wavelength causes functional changes in α . The measurement of α versus wavelength produces an ORD spectrum.

In order to observe circular dichroic spectra, one must be able to physically resolve linearly polarized light into the two circular components and detect a difference in the relative absorbance of each by the medium in question. In fact, it is the differential absorption that is measured in CD as well as the angle of rotation α . Therefore, samples must contain a chromophore to absorb, as well as be chiral, in order to observe an unequal absorption of the circularly polarized components. This differential absorption removes the equivalence of the vectors E_R and E_L , which forces the resultant rotating vector sum E to trace out an ellipse rather than lie in a single plane as before (Figure 7). The light leaving the chiral, absorbing medium is thus elliptically polarized and the material is said to exhibit circular dichroism.

The resulting ellipse can be characterized with the angle of ellipticity:

$$\psi = \tan^{-1}(a/b)$$

Eq. 2.3



Used by permission, E. D. Olsen, "Modern Optical Methods of Analysis", McGraw-Hill, 1975.

Figure 7. End View of Electric Field Vectors on Passage of Linearly Polarized Light Through an Optically Active Material. The Wavelength of Light is Near an Absorption Band.

where a and b are the minor and major axes of the ellipse as shown in Figure 7.

Just as the angle of rotation α was a function of the circular birefringence of the medium, the angle of ellipticity ψ is a function of the circular dichroism of the medium ($a_L - a_R$):

$$\psi = (\pi/\lambda)(a_L - a_R) \quad \text{Eq. 2.4}$$

where a_L and a_R are the molar absorptivities for the left and right circularly polarized rays respectively.

A more useful characterization of the ellipticity is the molar ellipticity θ , which is defined by:

$$\theta = (\psi/lC) \quad \text{Eq. 2.5}$$

where l is the cell path length in centimeters and C is the molar concentration of the absorbing species.

The similarity between Eq. 2.5 and the Beer-Lambert Law for absorption spectroscopy can be easily seen. Eq. 2.5 can be used to construct linear calibration curves of ψ versus C limited only by the experimental criteria for the limit of detection and excessive absorption. These calibration curves will have a slope equal to the molar ellipticity θ .

In practice, the angle of ellipticity ψ can only be measured indirectly by first measuring the absorption of each of the two circularly polarized rays and then taking the differences as described in Eq. 2.4. There must, therefore, be a method for producing alternating left and

right circularly polarized light rays. This is achieved by the use of an electro-optic modulator or quarter-wave plate. This device consists of a thin slice of a uniaxial crystal coated on both sides with a conductive material. When an electric field is applied to the crystal it becomes biaxial. This is known as the Pockel's effect and yields a quarter-wave (hence, the name) retardation of the light beam. The quarter-wave phase change causes the two rays to combine to form one circularly polarized wave. The polarity of the voltage is varied to change the light first into left and then into right circularly polarized light during the course of one cycle of the alternating voltage. The difference in the absorption during each cycle is measured and recorded. This difference measured as a function of wavelength produces the CD spectrum.

Although CD is primarily used for qualitative purposes, due to certain "fingerprint" characteristics found in the CD spectra, it can be used for quantitative purposes as well. The wavelengths where maxima (λ_{max}^+ , λ_{max}^-) and minima (λ_{min}^+ , λ_{min}^-) are observed are constant for a particular compound as well as the "crossover" wavelengths (λ_0). These "crossover" wavelengths are the wavelengths at which the sample medium is not circularly dichoric ($a_L = a_R$).

Due to the selectivity and sensitivity of CD, it has been used and has a bright future applied to the determination of biologically active compounds such as drugs, both

pharmaceutical and illicit, proteins and body fluids.

As in other types of absorption spectroscopy, CD spectra are subject to alterations due to solvent effects. As in other types of absorption spectroscopy, CD spectra are subject to alterations due to solvent effects. At first glance, this may seem to be a drawback to the method, but, in actuality, these effects afford us the opportunity to examine certain solvent-sample interactions. Solvation effects, pH effects, and solvent polarity all affect CD spectra by the same well known mechanisms that affect absorption spectra (19).

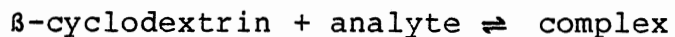
One particularly interesting exploitation of these effects is obtained via the use of chiral co-solutes which form a complex with the analyte compound. These complexes consist of two molecules, neither of which may fulfill the criteria for CD activity alone, but which together can produce a CD spectrum.

Cyclodextrin sugars have been shown to participate as host molecules in complexation with many different analytes (20). The cyclodextrins are produced by the action of *Bacillus Macerans* amylase on starch and are α -(1,4) linked D-glucose oligomers (21). The cyclodextrin rings of six (α), seven (β), or eight (γ) glucose residues have internal diameters ranging from six to ten angstroms (Figure 8).

The cyclodextrins abduct the analyte molecules in to their non-polar cavities to form inclusion complexes (Figure

9). The evidence for the formation of inclusion compounds in solution has been derived from kinetic and NMR data (22, 23). The hydrophobic interior of the cyclodextrin binds to a hydrophobic portion of the guest molecule, such as a benzene or pyridine ring. The complexes formed are usually 1:1 host to guest complexes (21).

By the use of established mathematical treatments for handling spectrophotometric data, the binding constant for the equilibrium :



can be calculated (24). The constants for many cyclodextrin-analyte systems have been previously reported (20, 21).

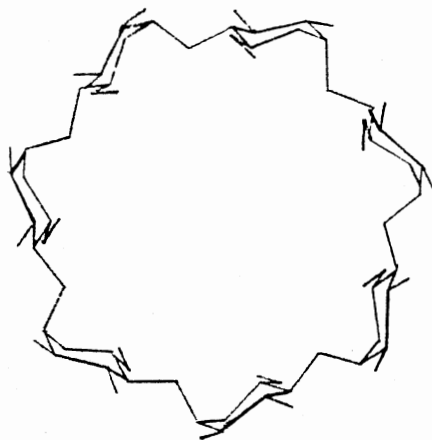


Figure 8. Ring Structure of β -cyclodextrin

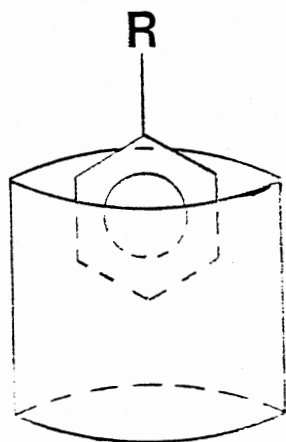


Figure 9. Schematic of an Inclusion Complex

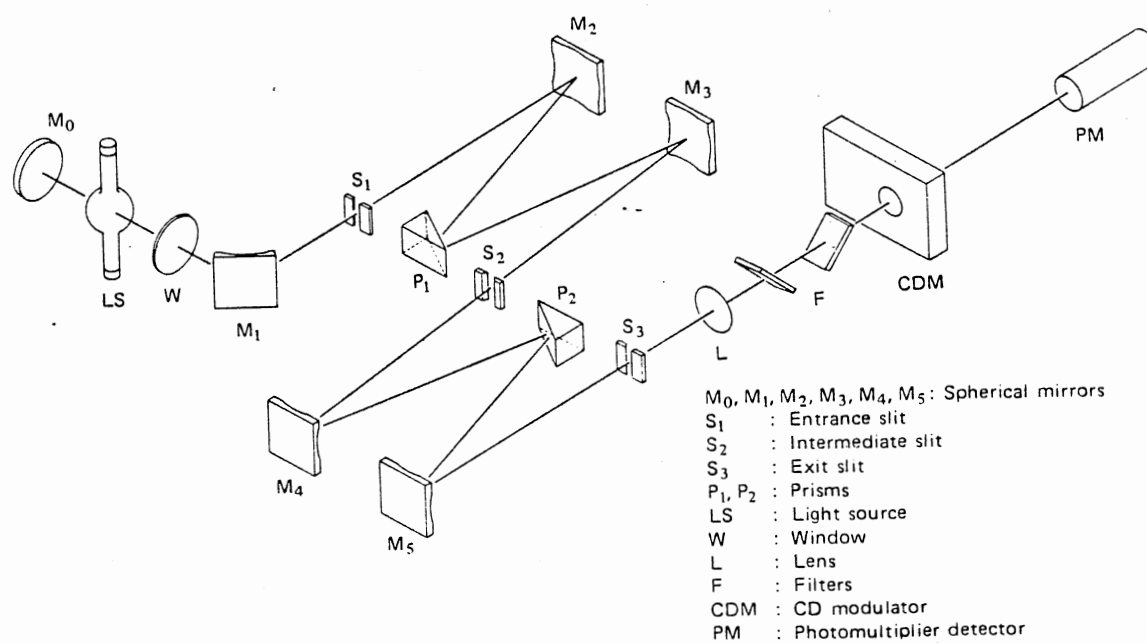
CHAPTER III

EXPERIMENTAL

Instrumental

All of the circular dichroic measurements were made on a JASCO (Japan Spectroscopic Company, Easton, Maryland) J-500A spectropolarimeter. This instrument is equipped with a JASCO DP-500N data processor which enables repeated scanning of the spectra at high scanning rates, spectral averaging, spectral smoothing, baseline subtraction, computer prediction of the CD spectra of mixtures, and many other operations.

The instrument has a wavelength range of 180 through 700 nanometers and a sensitivity scale from $0.1 \text{ m}^\circ \text{ cm}^{-1}$ to $100 \text{ m}^\circ \text{ cm}^{-1}$. The source is a 450 watt Xenon arc lamp which is water cooled to protect the instrument from the high temperatures of the arc. The optical system consists of a double prism monochromator to function both as a monochromator and a polarizer (Figure 10). The instrument is continuously purged with nitrogen gas, which is boiled from the liquid state for economic reasons. The nitrogen filled optical system removes any absorption due to oxygen and prevents any ozone production from the interaction of



Source: JASCO Incorporated (September 10, 1979)

Figure 10. Optical System of the JASCO J-500A Circular Dichroism Spectropolarimeter.

ultraviolet radiation with oxygen.

The ellipticity scale is calibrated daily using a 0.05% (w/v) androsterone/dioxane solution. The instrument is adjusted such that this solution produces 96.2 millimeters of deflection at 304 nanometers with the sensitivity set at $20 \text{ m}^\circ \text{ cm}^{-1}$. of chart paper using a 10 millimeter path length cell.

The cells used for the analyses were made from quartz crystal. Path lengths of 1 or 10 millimeters were used, determined by the concentration of the solution under study.

Two balances were used to weigh samples and standards. A CAHN (Cahn Instrument Company, Paramount, California) RG model 2000 electrobalance was used for mass measurements of samples weighing between 0 and 5 ± 0.05 milligrams. For larger samples a Sartorius (Sartorius-Werke AG, Germany) model 2403 laboratory balance was employed.

All of the extractions were done on a Lab-Line (Lab-Line Instrument Inc., Melrose Park, Illinois) Universal Oscillating shaker operating at approximately 42 oscillations per minute.

The calculation of binding constants and the linear regression analysis of the calibration curves were done on a HP-85A (Hewlett-Packard Intercontinental, Palo Alto, California) personal micro-computer. All software used in the calculations was written by the author.

Chemicals

The isotropic solvents were distilled water (buffered) and spectral grade organic reagents, which were used without further purification.

Standard nicotine and β -cyclodextrin were purchased from Kodak (Eastman-Kodak Company, Rochester, New York). Both were used without further purification steps. The cotinine was prepared by the oxidation of nicotine with an excess of hydrogen peroxide followed by treatment with sodium hydroxide to react with the remaining peroxide. The degree of oxidation was unknown but assumed to be 100%.

Smokeless tobacco samples were purchased, at random, from a local convenience store and kept under constant 81% relative humidity over a saturated solution of ammonium sulfate.

Experimental Procedures

Nicotine and cotinine standards are liquids at room temperature and were quantitatively transferred by "pipet-man" (Rainin Instrument Co. Inc., Woburn, MA) calibrated automatic delivery pipet dispensers. The model numbers used were P-20, P-200, and P-1000. Each was used according to the manufacturer's recommended operation procedure. Table III gives the manufacturer's reported accuracy and reproducibility figure for each of the three models.

Dilution series were prepared by successive dilutions of stock solutions of approximately 4×10^{-2} moles

TABLE III
RAININ PIPETMAN SPECIFICATIONS **

Model	Accuracy *	Reproducibility *
P-20	< 0.1 μ l @ 1-10 μ l < 1 % @ 10-20 μ l	< 0.04 μ l @ 2 μ l < 0.05 μ l @ 10 μ l < 0.06 μ l @ 20 μ l
P-200	< 0.5 μ l @ 20-60 μ l < 0.8 % @ 60-200 μ l	< 0.15 μ l @ 25 μ l < 0.25 μ l @ 100 μ l < 0.3 μ l @ 200 μ l
P-1000	< 3 μ l @ 100-375 μ l < 0.8 % @ 375-1000 μ l	< 0.6 μ l @ 250 μ l < 1.0 μ l @ 500 μ l < 1.3 μ l @ 1000 μ l

* Aqueous solutions, tips prerinsed once. ** Data obtained from Rainin Instrument Co. Inc.

per liter. Standard laboratory volumetric glassware was used without further calibration.

After proper mixing, the samples were placed in the cell compartment to equilibrate and the spectra were measured over the wavelength range of 230-320 nanometers in most cases. This range encompasses the majority of the nicotine and/or cotinine CD bands. The sensitivity used was dependent upon the cell path length and the concentration of the solution being assayed, but for most cases was either 2 or 5 millidegrees per centimeter of chart paper. The time constant was set at one second for all of the runs. The scan rate was fifty nanometers per minute and each sample was scanned four times.

By repeating the number of sample scans, the signal-to-noise ratio can be improved. This is accomplished by successive averaging of the signals for each scan. The noise is inversely proportional to the square root of the number of scans. This means that the noise in the data obtained from sixteen scans is one fourth of the noise in the data obtained from a single scan. It is left to the operator to decide, by consideration of the properties of the spectrum and the time consumed per scans, what number of scans is acceptable.

The data processor was used to subtract a recently obtained baseline spectrum from each sample spectrum prior to its being transferred to hard copy. The baseline was checked periodically in order to insure against any

instrumental drift.

The ellipticity versus concentration graphs were constructed in accordance with Eq. 2.5. The standard solutions for each of these graphs were prepared quantitatively from the stock solutions. Due to the pH effects in the respective spectra, all of the aqueous solutions were buffered at 8.2 ± 0.05 pH (pHydrion Buffers, Micro Essential Laboratory, Brooklyn 10, New York). All of the solutions in a particular series were run on the same day in an effort to minimize any day to day instrumental fluctuations that might occur.

Ellipticity maxima were measured directly from the chart paper with an expandable caliper. The linear regression for these data plotted versus solution concentration follow an algorithm that forces the y-intercept of the line through the origin, a condition required by Eq. 2.5 (see Appendix A).

CHAPTER IV

EXPERIMENTAL RESULTS

The primary goal of this work is the development of a simple, fast, and accurate method for the circular dichroic determination of nicotine, a task to which there is no reported precedent. Consequently, there is no basis for the comparison of the observed results.

The first need was to select a solvent system that would 1) efficiently extract the nicotine from the sample. 2) inefficiently extract any other circularly birefringent and/or absorbing species, 3) not participate in a pH reaction with nicotine and, 4) not absorb or produce any CD signal itself. Since the extraction process is one step that is common to many of the reported methods of nicotine analysis, the selection of a solvent system may be based upon reported results. Two solvent systems that are commonly used for the extraction of nicotine are isopropanol and dioxane-isopropanol mixtures. Pillsbury and Bright reported that there was no difference in the nicotine recovery by these two solvents. Thus, in the interest of simplicity, reagent grade isopropanol was chosen as the preferred solvent (25). This choice coincided well with each of the listed criteria for a satisfactory solvent system.

The Circular Dichroic Spectrum of Nicotine

The CD spectrum of nicotine in isopropanol shows the typical aromatic triplet observed in UV absorption between 245 and 270 nanometers (Figure 11). The third peak of the triplet, at 246 nanometers, is reduced to a shoulder of the 255 nanometer peak and was not considered for quantization. The wavelengths of the useful negative maxima (λ_{max}^-) are at 261 and 255 nanometers respectively. The molar ellipticities (θ) for these maxima are -87.61 and -77.83 degrees of ellipticity per molar solution per centimeter path length respectively. A positive band whose maximum (λ_{max}^+) occurs at 236 nanometers was found to have a molar ellipticity of +41.04 degrees per molar solution per centimeter path length. These and other spectral characteristics for nicotine are included in Table IV.

Linear Dynamic Range for Nicotine

Theoretically, each wavelength will obey the Beer's law type relationship given by Eq. 2.5. The common practice, however, is to collect data at the wavelength maxima (+ or -), where the slope of the spectrum is near zero, instead of at wavelengths where the error in the measurement of the signal height is enhanced due to a steep slope in the spectrum. The calibration curves of observed ellipticity versus concentration for each of the wavelength maxima in the nicotine spectrum along with the respective linear regression statistics are shown in Figures 12-14. The

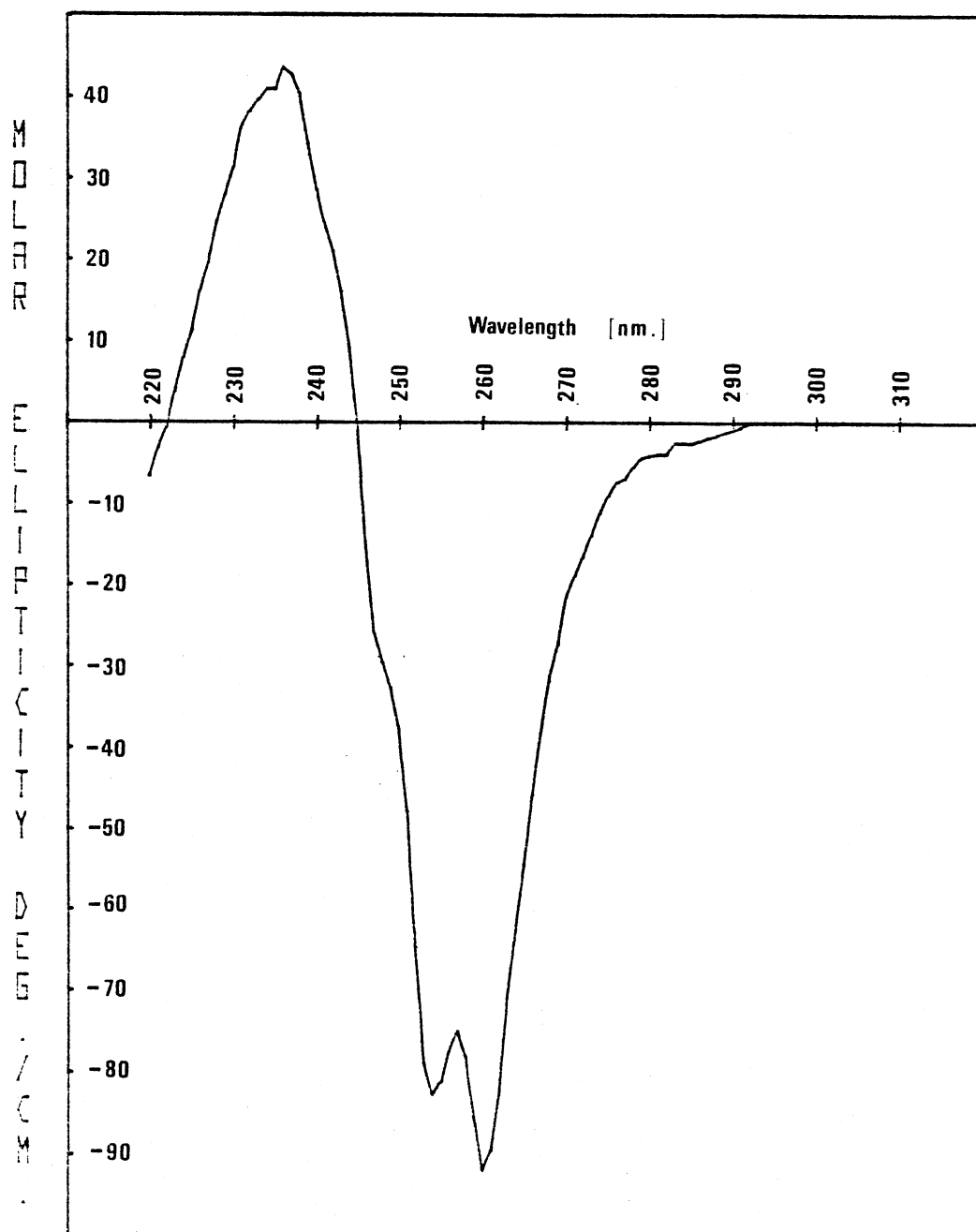
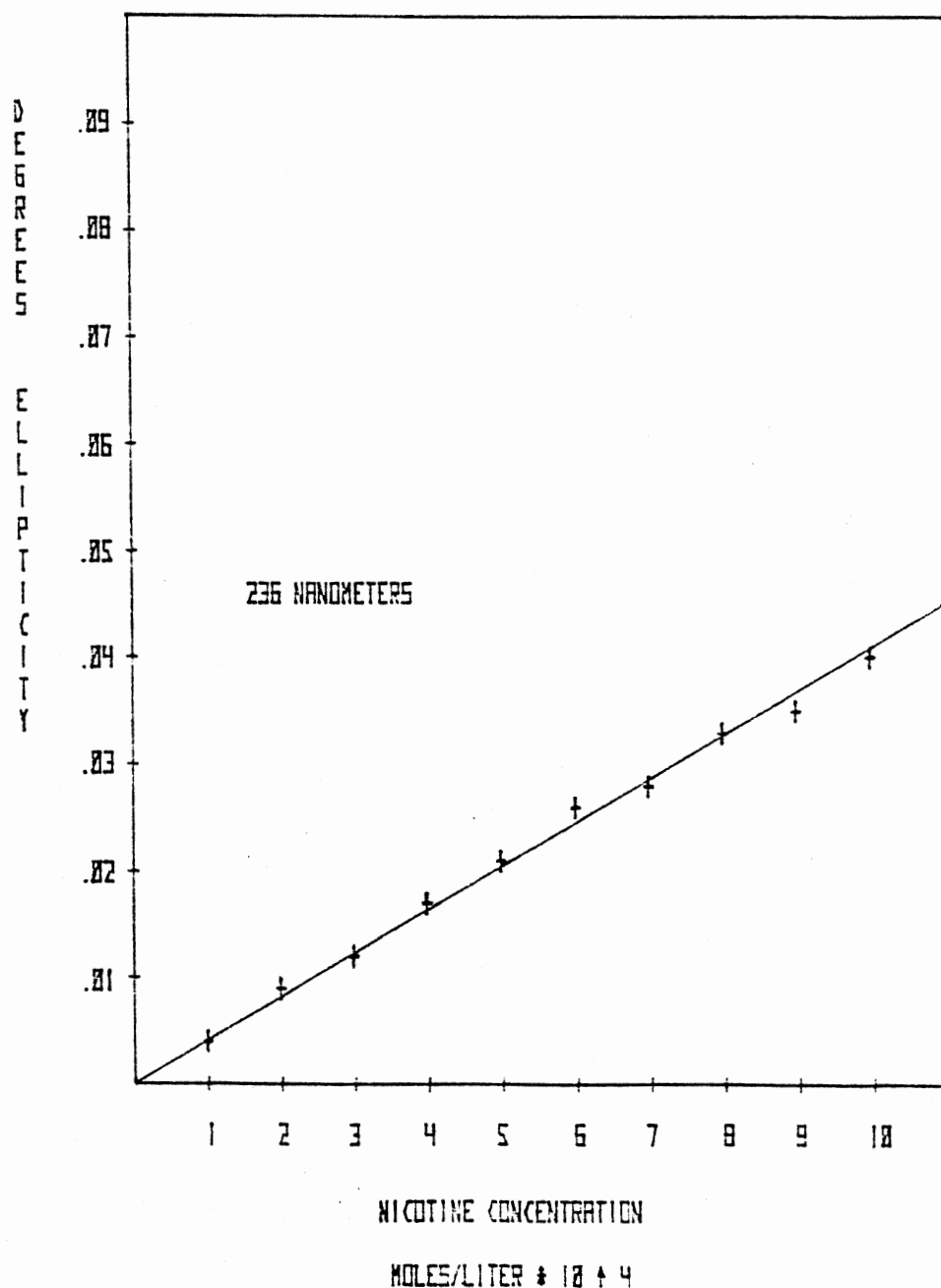


Figure 11. The Isopropanoic Circular Dichroic Spectra of Nicotine

TABLE IV
CD SPECTRAL CHARACTERISTICS OF NICOTINE

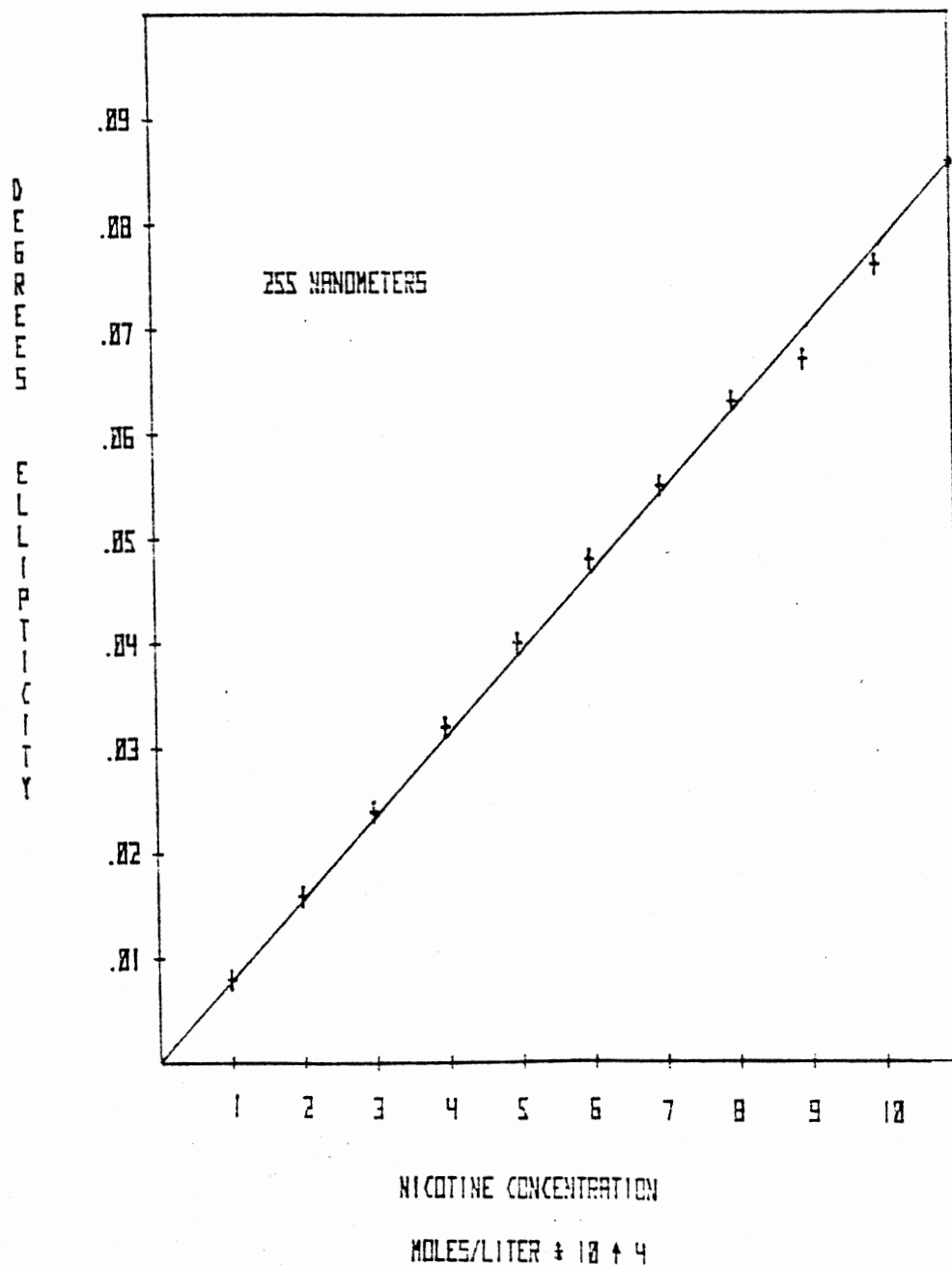
Characteristic	Wavelength (nm)	Molar Ellip. °M ⁻¹ cm ⁻¹
λ_{max}^-	255	-77.83 *
λ_{max}^-	261	-87.61 *
λ_{max}^+	236	+41.04 *
λ_{min}^-	257	- - -
λ_0	244	0.00 **
λ_0	222	0.00 **

* From the slope of ellipticity versus concentration linear regression analysis (Figures 12-14). ** By definition.



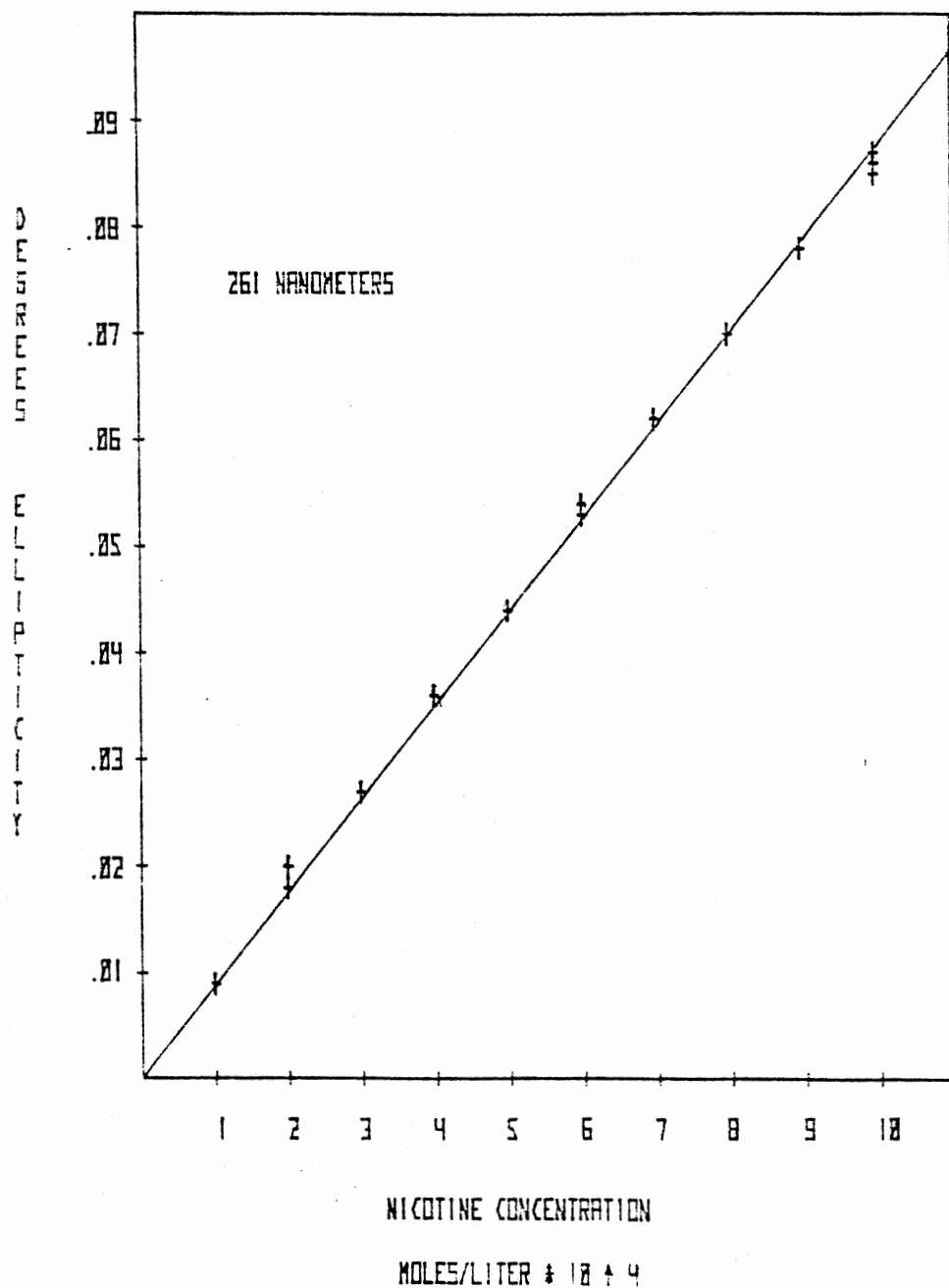
Slope = θ = 77.82 degrees per molar solution per centimeter.
 Correlation Coefficient (r^2) = 0.999. Standard deviation
 of the slope = $1.03 \times 10^{-1} \text{ M}^{-1} \text{ cm}^{-1}$.

Figure 12. Absolute Value of Observed Ellipticity Versus
 Nicotine Concentration Calibration Curve and
 Linear Regression Statistics. Solvent: Iso-
 propanol



Slope = θ = 77.82 degrees per molar solution per centimeter.
 Correlation Coefficient (r^2) = 0.999. Standard deviation
 of the slope = 1.03×10^{-4} M⁻¹cm⁻¹.

Figure 13. Absolute Value of Observed Ellipticity Versus Nicotine Concentration Calibration Curve and Linear Regression Statistics. Solvent: Iso-propanol



Slope = θ = 87.61 degrees per molar solution per centimeter.
 Correlation Coefficient (r^2) = 0.999. Standard deviation
 of the slope = $1.64 \times 10^{-1} \text{ M}^{-1} \text{ cm}^{-1}$.

Figure 14. Absolute Value of Observed Ellipticity Versus Nicotine Concentration Calibration Curve and Linear Regression Statistics. Solvent: Iso-propanol

solvent is isopropanol.

In circular dichroism, the upper limit applied to a calibration curve is a function of the absorbance by the sample and the sample matrix. For nicotine solutions in isopropanol this limit is approximately 1×10^{-3} moles per liter in a 10 millimeter path length cell.

The lower limit to the calibration curve can be defined as the minimum detectable quantity (MDQ). The MDQ is determined by a minimum acceptable signal-to-noise ratio. One method of calculating the MDQ is known as Kaiser's limit of detection (26).

Kaiser's limit of detection can be calculated by:

$$\psi_{MDQ}(\lambda) = \langle \psi_N(\lambda) \rangle + 3 \cdot s_N(\lambda) \quad \text{Eq. 4.1}$$

where: $\psi_{MDQ}(\lambda)$ is the observed ellipticity of the MDQ at wavelength λ .

$\langle \psi_N(\lambda) \rangle$ is the average ellipticity of the noise from solvent spectra at wavelength λ .

$s_N(\lambda)$ is the standard deviation of the noise from solvent spectra at wave length λ .

$\langle \psi_N(\lambda) \rangle$ and $s_N(\lambda)$ are calculated from the noise in the data of 20 solvent spectra. Since the noise is a function of wavelength, so too are $\langle \psi_N(\lambda) \rangle$ and $s_N(\lambda)$; therefore, $\psi_{MDQ}(\lambda)$ must be calculated for each of the wavelengths to be used. Once $\psi_{MDQ}(\lambda)$ has been determined, the MDQ is calculated using a variation of Eq. 2.5:

$$MDQ(\lambda) = \psi_{MDQ}(\lambda) / (b * \theta(\lambda)) \quad \text{Eq. 4.2}$$

where: $MDQ(\lambda)$ is the minimum detectable quantity at wavelength λ in moles per liter.

b is the cell path length in centimeters.

$\theta(\lambda)$ is the molar ellipticity in degrees per molar solution per centimeter path length at wavelength λ .

It should be noted that the MDQ is a function of wavelength and is minimized at the wavelengths having the highest θ values, except when the noise level causes $\langle \psi_N(\lambda) \rangle$ and $s_N(\lambda)$ to be excessively large. Using Kaiser's limit of detection, the MDQ is a function of the solvent and the sensitivity of the CD measurement upon the analyte in question. Table V lists the Kaiser's limits of detection for isopropanol solutions of nicotine versus wavelength.

Determination of Nicotine in Smokeless Tobaccos

Various smokeless tobacco brands were chosen as test samples because of their increasing popularity among American tobacco users, and because of the lack of evidence in the literature for analytical determinations of the nicotine content in these mixtures (1).

In view of the criteria involved in the production of a CD spectrum, other separation and/or concentration steps may not be required in the workup procedure of the extract solution. Species that present problems in other methods

TABLE V

KIASER'S LIMIT OF DETECTION FOR ISOPROPANIOC NICOTINE SOLUTIONS
AT 236, 255, AND 261 NANOMETERS

Wavelength	$\langle \gamma_N(\lambda) \rangle$	$s_N(\lambda)$	$\gamma_{MDQ}(\lambda)$	Limit of Detection
236 nm.	$1.10 \times 10^{(-4)^\circ}$	$2.04 \times 10^{(-5)^\circ}$	$1.71 \times 10^{(-4)^\circ}$	$4.17 \times 10^{(-6)}_M$
255 nm.	$7.41 \times 10^{(-5)^\circ}$	$1.14 \times 10^{(-5)^\circ}$	$1.08 \times 10^{(-4)^\circ}$	$1.39 \times 10^{(-6)}_M$
261 nm.	$6.50 \times 10^{(-5)^\circ}$	$9.78 \times 10^{(-6)^\circ}$	$9.43 \times 10^{(-5)^\circ}$	$1.08 \times 10^{(-6)}_M$

are non-interfering and therefore do not need to be removed. The UV spectrum of a tobacco extract when compared to the UV spectrum of pure nicotine, demonstrates that there are species present that would require removal if UV spectroscopy were the chosen method of analysis (Figure 15). In contrast, when a comparison of the CD spectra of these solutions is made the interfering species do not present a problem (Figure 16). Therefore, determinations can be obtained directly from the measurements made on the extract solutions.

Since we proposed to report results as a weight percent nicotine we felt it was important to control the sample humidity. It was first decided that representative samples taken from the bulk should be dried prior to weighing. Samples were dried over phosphorus pentoxide (Sargent-Welch) overnight. Spectra were readily reproducible among samples taken from the population. In a comparative study, extractions were made from moist samples taken from the same population. It was found that the extraction efficiency of nicotine decreased by approximately a factor of ten when the samples were dehydrated before extraction. The reason for this phenomenon was not of momentary interest and another alternative, that of equilibration at constant humidity, was tested. A saturated ammonium sulfate (Malinckrodt) was used to keep the samples at constant 81% relative humidity throughout storage. Ammonium sulfate was chosen because of a reported relatively constant humidity capacity of $\pm 0.1\%$

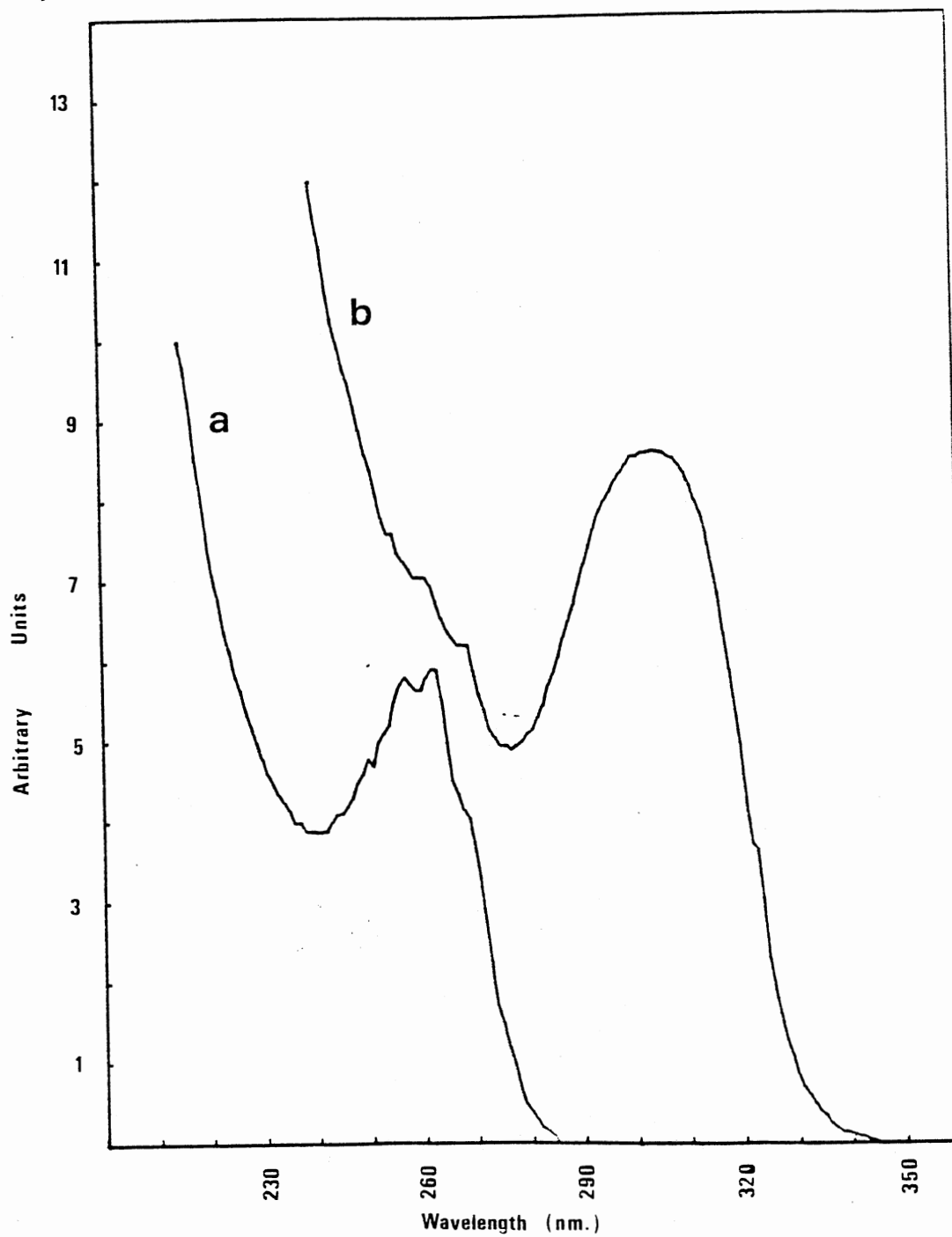


Figure 15. The UV Spectra of a) Pure Nicotine and b) The Extract From a Smokeless Tobacco Sample

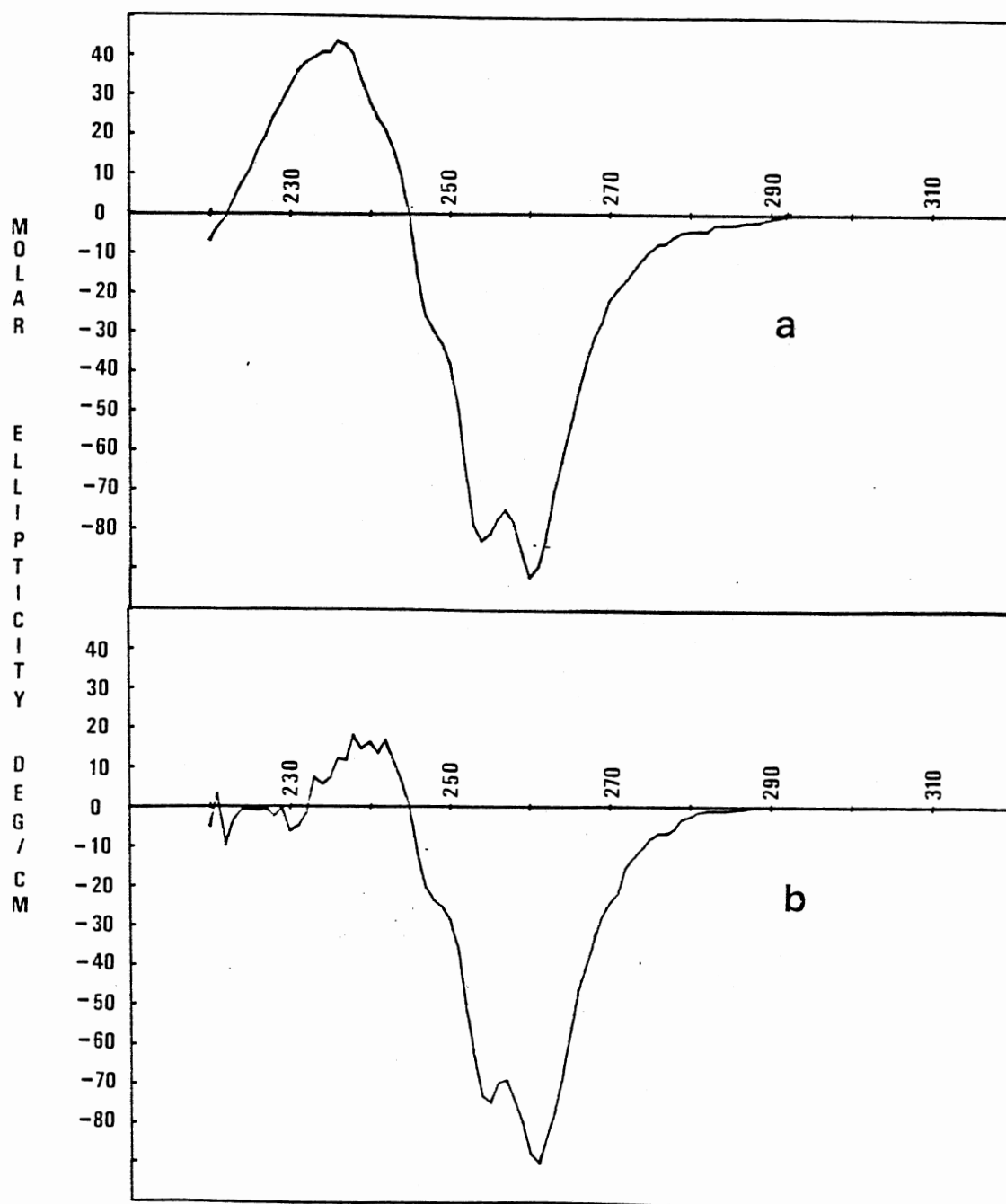


Figure 16. The CD Spectra of a) Pure Nicotine and b) The Extract From a Smokeless Tobacco Sample

at 25 ± 5 °C (27).

The optimum extraction time, consistent with sample turn around time, was determined by the analysis of SKOAL (U.S. Tobacco Co.) samples. Each .1-.2 gram specimen was extracted into 5 milliliters of isopropanol by agitation on a constant speed oscillating laboratory shaker. The samples were subjected to different extraction times ranging from one to sixty-four minutes. A plot of the percent nicotine by weight calculated from the CD data versus extraction time is presented in Figure 17. Thirty minutes of solvent contact is of sufficient duration to effectively remove all of the extractable nicotine from the sample.

In order to determine what percent of the total nicotine was represented by this extraction, similar sample weights were placed in the thimble of a Soxhlet extractor and washed with distilled isopropanol for a period of 18 hours. In this way an infinite extraction is approximated. Comparision of the results from both extraction procedures indicated that the extended extraction time coupled with the elevated extraction temperature provided in the Soxhlet apparatus afforded no additional nicotine recovery. This information, along with the unknown mechanism by which the nicotine is bound to the tobacco leaf, left the mandatory assumption that, after 30 minutes of extraction, the nicotine recovery was conceivably 100 percent.

From the data used to compile Figure 17 (Table VI) and the 30 minute extraction time, it was determined that the

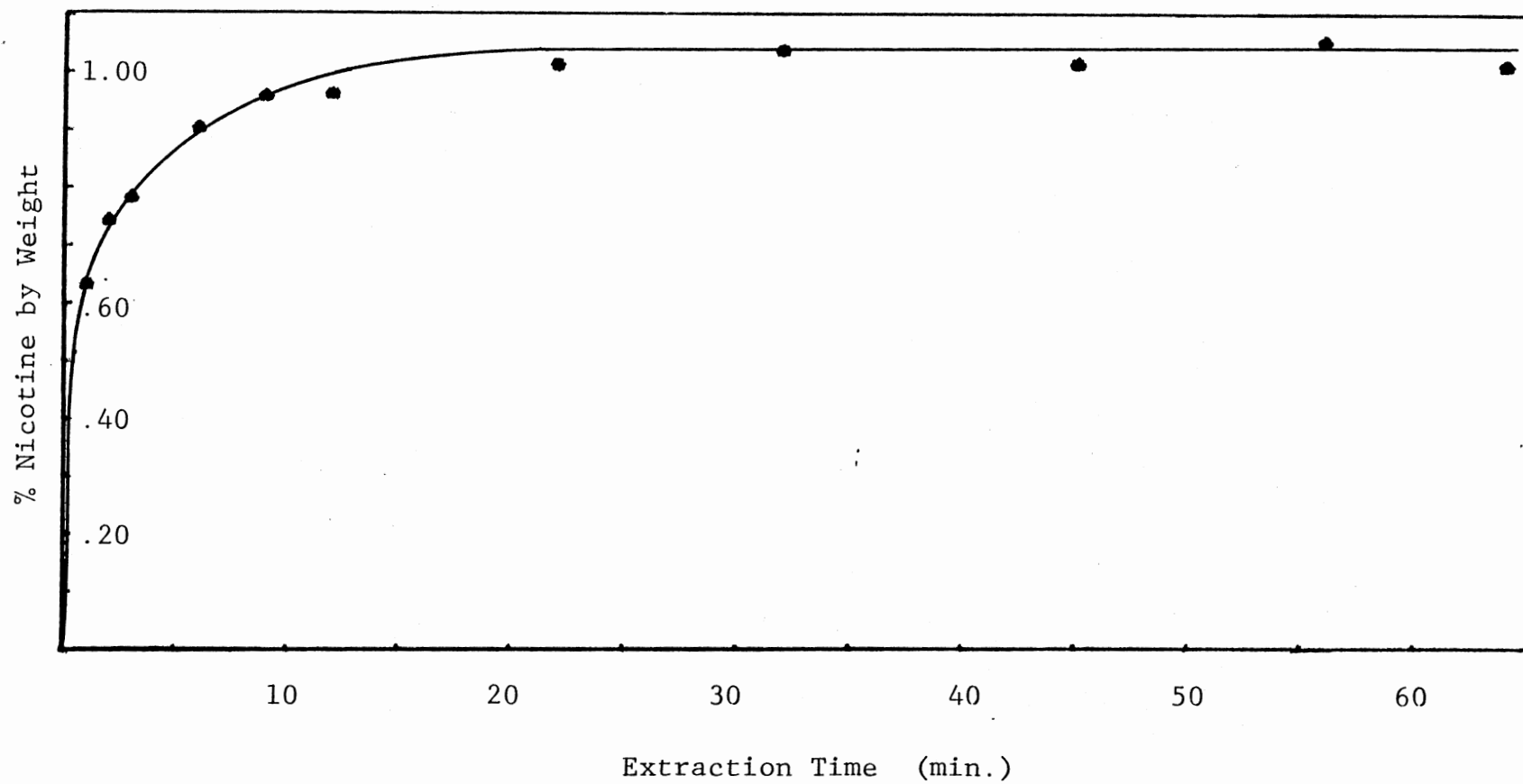


Figure 17. Percent Nicotine by Weight in SKOAL Versus Extraction Time

TABLE VI
PERCENT NICOTINE BY WEIGHT IN SKOAL
VERSUS EXTRACTION TIME DATA

Sample Weight (g)	Extraction Time (min.)	% nicotine by wt.
0.1904	1.00	0.6338
0.2396	2.00	0.7437
0.2515	3.00	0.7825
0.2801	6.00	0.9030
0.2601	9.00	0.9578
0.2616	12.00	0.9625
0.3333	22.00	1.0125
0.2147	32.00	1.0360
0.2010	45.00	1.0100
0.2062	56.00	1.0470
0.2349	64.00	1.0050

From last five data points: Average % nicotine by weight: 1.0221% . Standard deviation of same: $1.83 \times 10^{-2}\%$

percent nicotine by weight in 81% humidified SKOAL samples was $1.02 \pm 0.05\%$ with 95% confidence.

Triplicate samples of each of the three other popular smokeless tobacco brands were analyzed using the same procedure. Results for these analyses are given in Table VII.

Of the four smokeless tobacco brands, all are finely ground except for the HAWKEN (Conwood Tobacco Co.) variety. The size of the HAWKEN "particles" is approximately 10-15 times larger than those of the other respective brands. Upon extraction of the larger granules, the tobacco became dehydrated and brittle. The relatively low yields of nicotine from the HAWKEN samples are attributed to this factor, although the specifics were not determined. This observation does, however, suggest a possible correlation between extraction efficiency and surface area, which is not altogether unexpected.

Calculation of β - cyclodextrin -
nicotine constant (K_{bind})

The analytical procedure for determining the association/binding constant K_{bind} between β -cyclodextrin sugar and nicotine, in a one to one complex, involves the use of aqueous solutions and, therefore, is subject to pH effects. A change in the total nicotine concentration causes a large enough change in the pH of an unbuffered aqueous solution to affect the observed ellipticity of the

TABLE VII
SMOKELESS TOBACCO NICOTINE ANALYSIS RESULTS*

Brand	% nicotine by wt.	Ave. % nicotine	Stand. dev. % nicotine
SKOAL U.S. Tobacco Co.	Trial 1 : 1.0125 2 : 1.0360 3 : 1.0100 4 : 1.0470 5 : 1.0050	1.0221	$1.83 \times 10^{(-2)}$
HAWKEN	Trial 1 : 0.0624 2 : 0.0566 3 : 0.0632	0.0670	$3.42 \times 10^{(-3)}$
KODIAK Conwood Tobacco Co.	Trial 1 : 0.4946 2 : 0.4903 3 : 0.4927	0.4925	$2.43 \times 10^{(-2)}$
SILVERCREEK Silvercreek Tobacco Co.	Trial 1 : 1.0266 2 : 1.1632 3 : 1.1134	1.1011	$7.63 \times 10^{(-2)}$

* % nicotine by weight results are averages from determinations calculated at 255 and 261 nanometers.

CD spectrum. Table VIII shows the pH change corresponding to changes in the total nicotine concentration of the solution.

TABLE VIII
pH CHANGE IN AN UNBUFFERED AQUEOUS SOLUTION
CORRESPONDING TO TOTAL NICOTINE
CONCENTRATION CHANGES

[Total Nicotine] (M^{-1})	pH
1.215×10^{-6}	8.10
3.957×10^{-6}	8.60
1.272×10^{-5}	9.10
4.151×10^{-5}	9.60
1.432×10^{-4}	10.10
5.718×10^{-4}	10.60
2.997×10^{-3}	11.10
2.136×10^{-2}	11.60

* The values were calculated without respect to activities

The concentration range depicted in Table VIII embraces the total nicotine concentration that can be analyzed by circular dichroism. This range is governed by the factors that limited the calibration curves mentioned earlier. When the corresponding pH range is compared to an α (fraction of species) versus pH diagram for nicotine it can be seen that

the second pK region has been traversed, thus causing the predominant species to change from the free base (N) to the monoprotic species (HN^+) (Figure 18).

This information coupled with the probability that the two species have different molar ellipticity values, accounts for the changes observed in the CD spectra of unbuffered aqueous nicotine solutions caused by a change in the total nicotine concentration.

The obvious solution to this problem is to buffer the aqueous solution, thereby maintaining a constant ratio between the concentration of the two species. As the α versus pH diagram indicates, this ratio is constant at any pH, but, in the interest of obtaining predominantly one species, a buffer pH of 8.2 was chosen for the complexation study. The CD spectral characteristics for an 8.2 pH buffered aqueous nicotine solution are shown in Table IX.

The treatments which form the bases for the mathematical expressions for calculating association/binding constants assume that the molar ellipticities of the uncomplexed and complexed species are constant, though not necessarily equal, under constant physical conditions, and that the observed ellipticities are directly related to the concentrations of all of the circularly birefringent absorbing species.

Binding constants have been reported for β -cyclodextrin (β CD) - cocaine and β CD - PCP complexes (14). The method used to calculate the K_{bind} values involved an

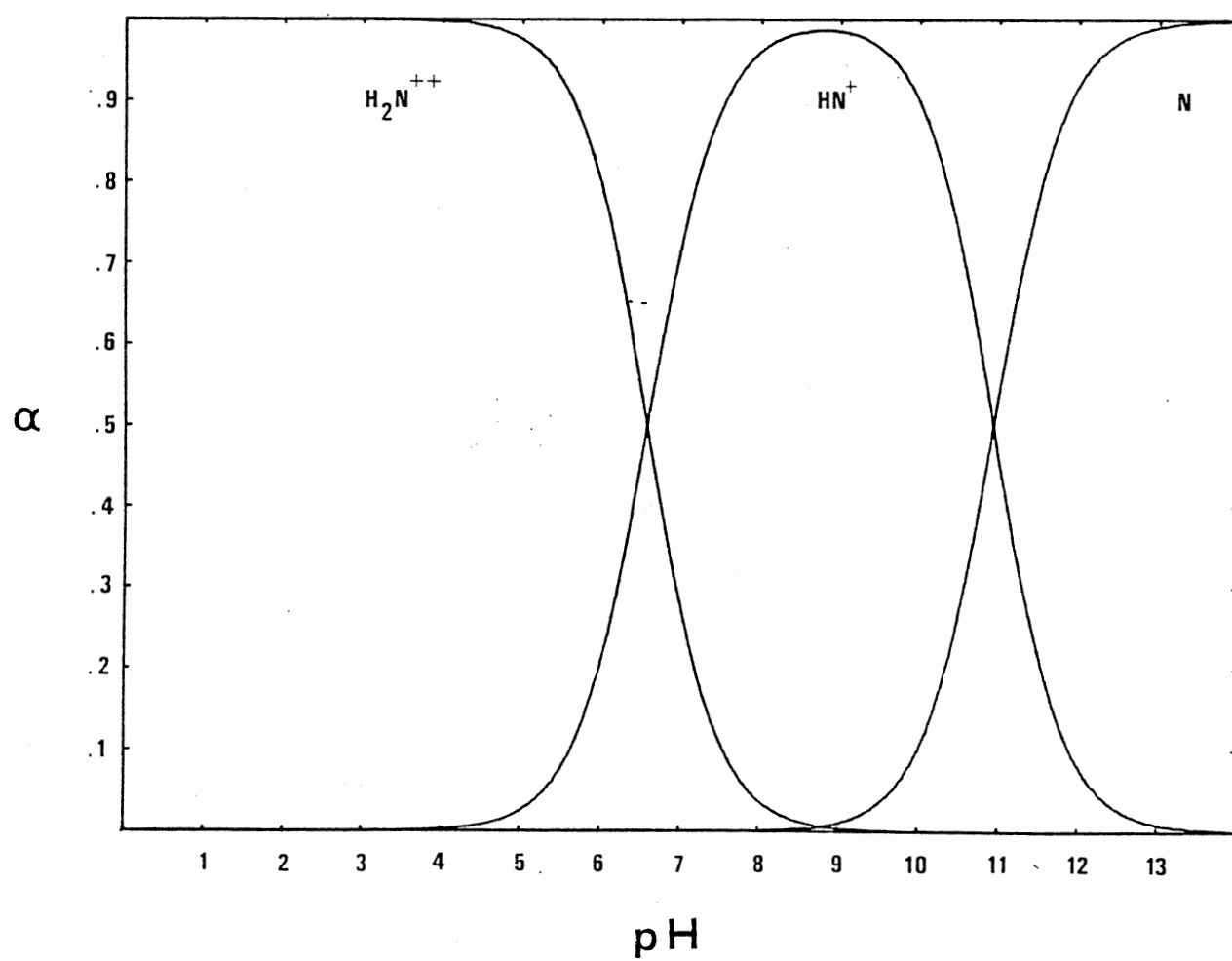


Figure 18. α Versus pH Diagram for Nicotine

TABLE IX
SPECTRAL CHARACTERISTICS OF 8.2 pH BUFFERED
NICOTINE SOLUTIONS

Characteristic	Wavelength (nm.)	Molar Ellipticity (°/M cm)
λ_{max}^-	264	- 64.40
λ_{max}^-	268	- 60.02
λ_{max}^+	240	+ 24.97
λ_{min}^-	266	----
λ_0	220	0.00*
λ_0	249	0.00*

* by definition.

educated guess of the molar ellipticity of the complex at the wavelength where the data were measured. This guess was used to calculate a K_{bind} value for each of several β CD concentrations. When the molar ellipticity was found that gave an equivalent K_{bind} at every β CD concentration the calculation was assumed complete and the results reported. In order to avoid the step of arbitrarily choosing the molar ellipticity of the complex and proceeding with a protracted reiterative calculation, another method was used (24).

Using the equation:

$$\frac{b[\beta\text{CD}][\text{TN}]}{(\psi_{\text{C}} - \psi_{\text{N}})} = \frac{([\beta\text{CD}] + [\text{TN}] - X)}{(\theta_{\text{C}} - \theta_{\text{N}})} + \frac{K'}{(\theta_{\text{C}} - \theta_{\text{N}})} \quad \text{Eq. 3.3}$$

where: b = the cell path-length in cm.

$[\beta\text{CD}]$ = the molar concentration of the β CD.

$[\text{TN}]$ = the molar concentration of nicotine.

ψ_{C} = the observed ellipticity of the β CD - nicotine solution in degrees.

ψ_{N} = the observed ellipticity of nicotine alone in degrees.

$\theta_{\text{C}}, \theta_{\text{N}}$ = the molar ellipticities of the complex and the nicotine alone respectively in degrees/Mcm.

X = the molar concentration of the β CD - nicotine complex.

K' = the dissociation constant for the complex K'
 $= (1/K_{\text{bind}})$.

the value for the binding constant ($K_{\text{bind}} = 1/K'$) and the molar ellipticity of the complex can be obtained. Data are collected by measuring the difference in peak heights which accompany increases in the β CD concentration. The nicotine concentration is kept constant throughout the analysis. Since β CD alone does not produce a CD signal, the change in the CD spectra can only be attributed to the formation of a chiral complex.

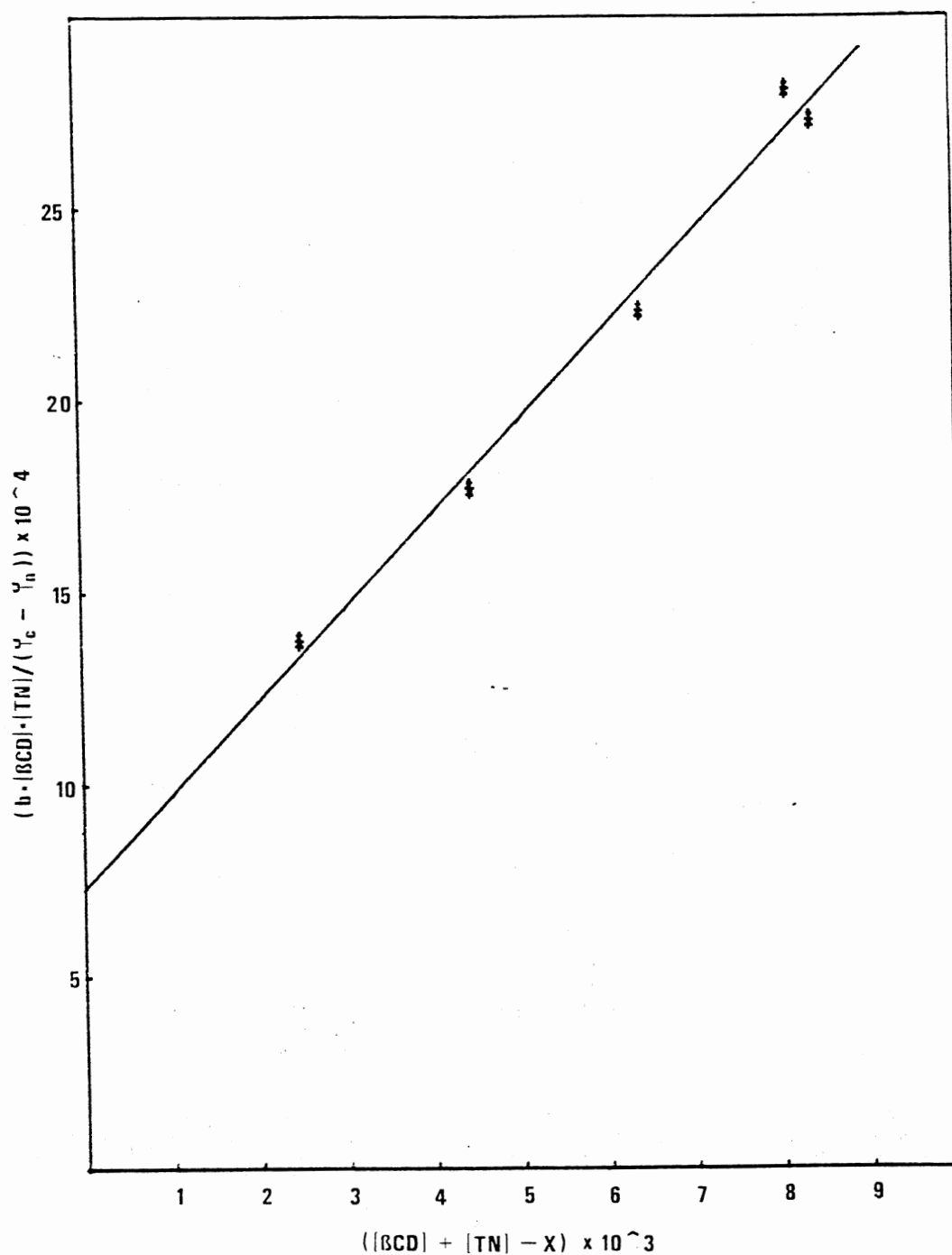
When $b[\beta\text{CD}] [\text{TN}]/(\theta_{\text{C}} - \theta_{\text{N}})$ is plotted versus $([\beta\text{CD}] + [\text{TN}] - X)$, ignoring the X values in the first approximation of Eq. 3.3, the slope is equal to $1/(\theta_{\text{C}} - \theta_{\text{N}})$ and the y-intercept is equal to $K'/(\theta_{\text{C}} - \theta_{\text{N}})$.

From the first approximation of the slope, X values are calculated for each solution in the series by solving the following quadratic equation:

$$X^2 - ([\text{TN}] + [\beta\text{CD}] - K')X + [\beta\text{CD}] [\text{TN}] = 0 \quad \text{Eq. 3.4}$$

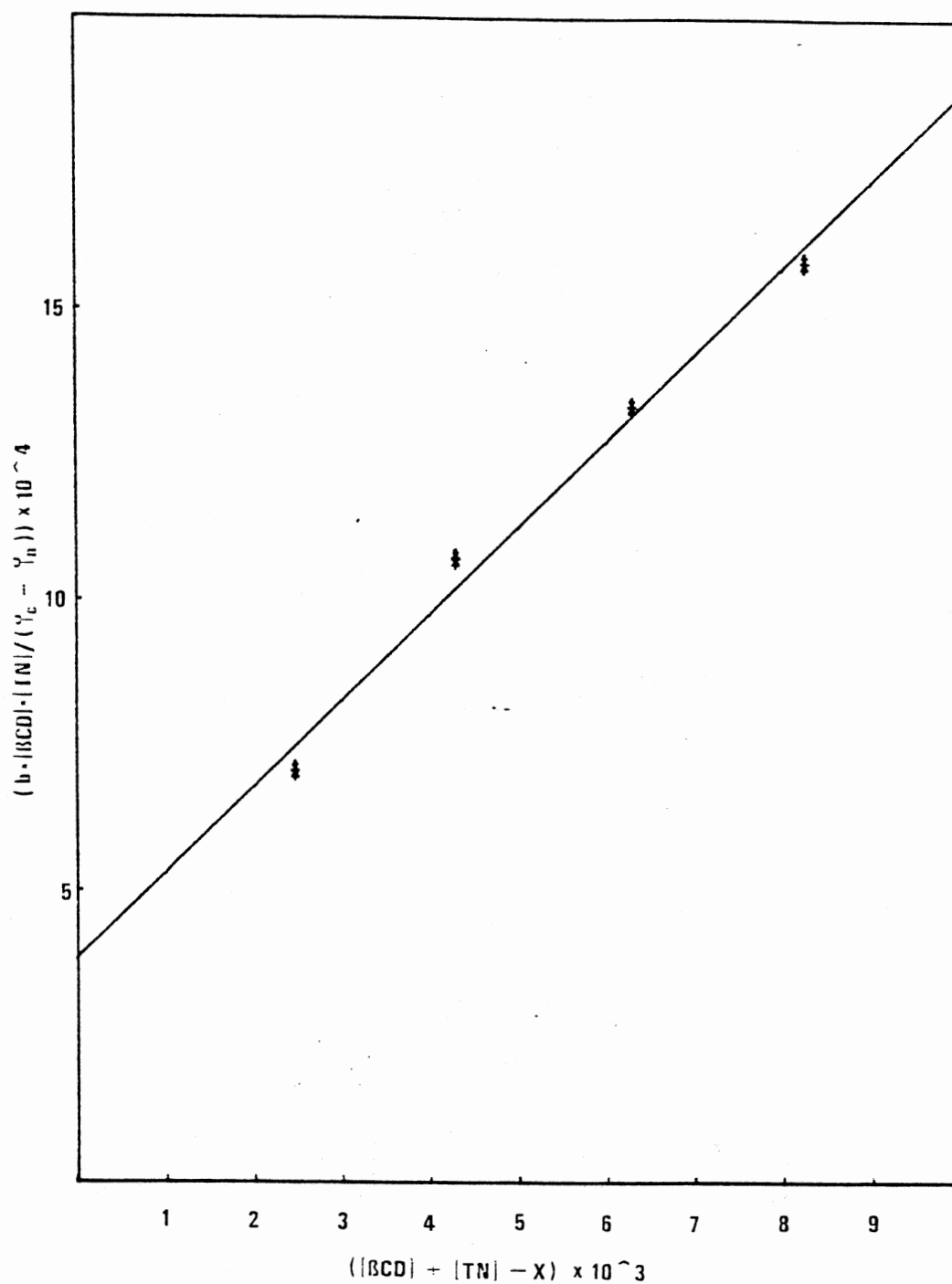
These values in turn are used to derive better estimates of the slope and y-intercept. The reiterative procedure is continued until the values for K' and θ_{C} are constant. Representative plots of Equation 3.3 for 264 and 268 nanometers are shown in Figures 19 and 20.

The values obtained for the molar ellipticities of the complex are -71.2 $^{\circ}/\text{M cm.}$ and -64.1 $^{\circ}/\text{M cm.}$ for the 264 and 268 nanometer maxima respectively. The average K_{bind} calculated from data for the wavelengths treated separately is 358.4. The confidence in these values is limited by the



Slope = $2.4821 \times 10^{(-1)}$. Intercept = $7.2893 \times 10^{(-4)}$.
 Molar Ellipticity of Complex = $-64.1 \text{ } ^\circ\text{M}^{-1}\text{cm}^{-1}$.
 $K_{\text{bind}} = 333$

Figure 19. Plot of Equation 3.3 for 268 Nanometers With Linear Regression Statistics



Slope = $1.4744 \times 10^{(-1)}$. Intercept = $3.8393 \times 10^{(-4)}$.
 Molar Ellipticity of Complex = $-71.2^\circ \text{ M}^{-1} \text{ cm}^{-1}$.
 $K_{\text{bind}} = 384$

Figure 20. Plot of Equation 3.3 for 261 Nanometers With Linear Regression Statistics

small difference in the molar ellipticity values of nicotine and the β CD-nicotine complex. The small difference together with the low nicotine concentrations that can be analyzed with CD, manifest relatively small changes in the overall CD spectrum of the solution. The error induced by the measurement of these small changes is carried through the calculation. It is hoped that these errors have been minimized by the linear regression that is applied to the plots from which the values are obtained.

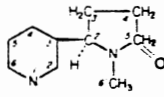
Determination of Cotinine

Cotinine, the major metabolite of nicotine, was first described in 1893 by Pinner (28). The structure of cotinine was confirmed by Frankenburg and Vaitekunas (29). It is formed by the oxidation of nicotine by hydrogen peroxide and/or UV light (29). Table X gives a summary of the properties of cotinine.

The cotinine used for this analysis was made by mixing nicotine with 30% hydrogen peroxide (Fisher Sci. Co.) in a 1:1 ratio. The mixture was allowed to stand over a three day period to achieve complete oxidation. The solution was made alkaline in order to remove any unreacted peroxide. Quantitative dilution series were made using 8.2 pH buffer as solvent.

The CD spectrum of cotinine is essentially a visual mirror image of the nicotine spectrum with molar ellipticity values that are reduced by a factor of approximately six

TABLE X
PROPERTIES OF COTININE

Structure	
IUPAC name:	(S)-1-Methyl-5-(3-pyridinyl)-2-pyrrolidinone
Formula:	$C_{10}H_{12}N_2O$
Molecular Weight:	176.21 g / mole
Boiling Point:	210-211°C (6 torr)
Description:	Viscous oil

Source: Merck Index 9th Edition.

TABLE XI
CIRCULAR DICHROIC CHARACTERISTICS OF
COTININE IN pH 8.2

Characteristic	Wavelength (nm.)	Molar Ellipticity (°/M cm)
λ_{\max}^+	261	+ 10.73
λ_{\max}^+	268	+ 10.60
λ_{\max}^-	243	- 1.80
λ_{\min}^+	264	----
λ_0	224	0.00*
λ_0	237	0.00*
λ_0	247	0.00*

* by definition.

(Figure 21). The spectral characteristics of the cotinine CD spectrum are listed in Table XI.

Due to the relatively small molar ellipticity of the 243 nanometer maximum, it has not been considered for quantization. The two positive maxima, however, can be used for quantitative purposes and the calibration curves for these two wavelengths are shown in Figures 22 and 23 along with the appropriate linear regression statistics.

Since the majority of the nicotine that is excreted from the body, via the urinary tract, is in the form of cotinine, the determination of binary mixtures of cotinine and nicotine is of some interest. Unfortunately, due to the much smaller molar ellipticities of cotinine compared to nicotine and the fact that the spectra are almost mirror images of one another, determinations of both components in a binary mixture are difficult to perform. Therefore, a procedure for the determination of binary nicotine and cotinine mixtures would require that steps be taken to separate the two species. Once the separation was achieved, the subsequent analysis could be done following conventional procedures.

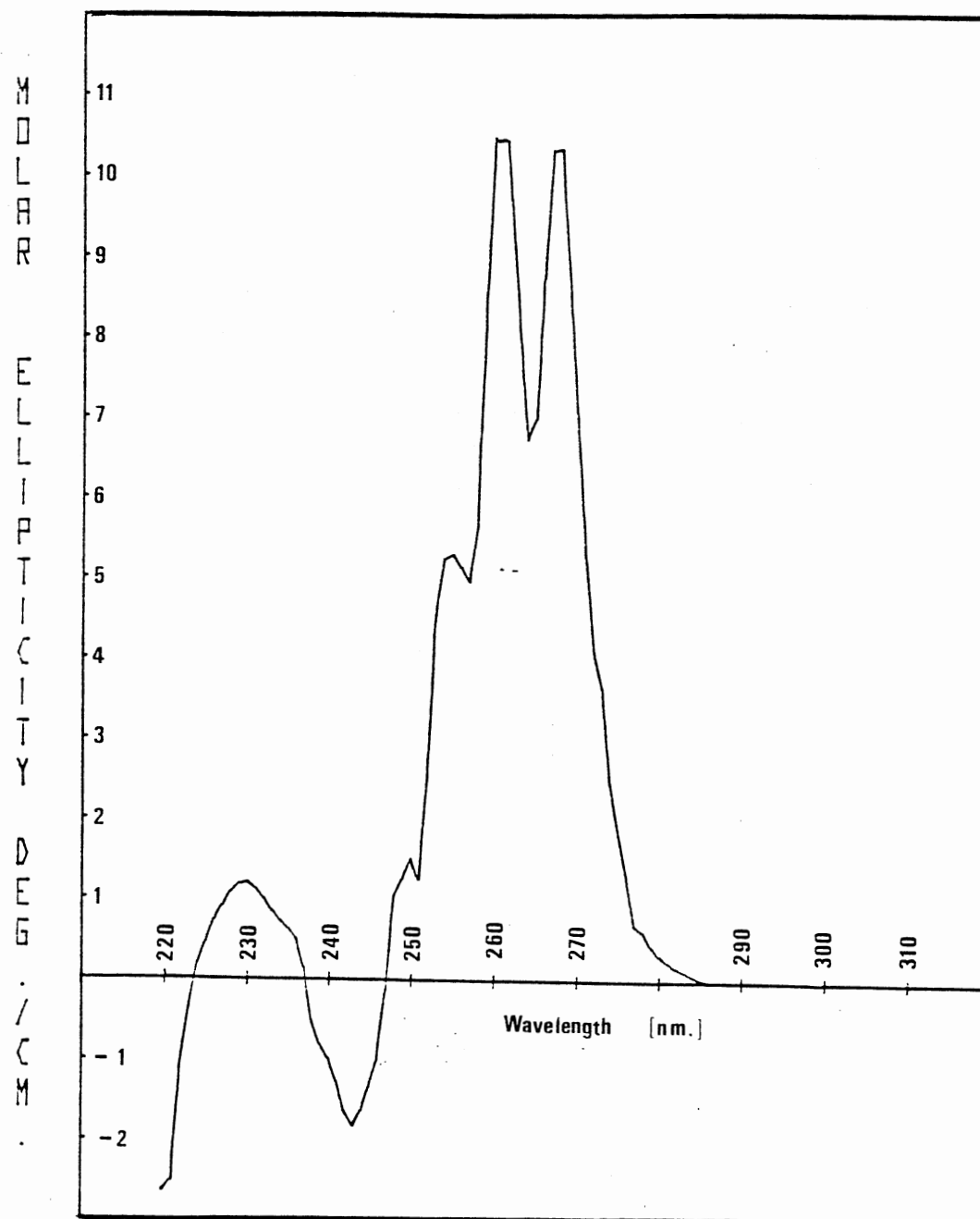
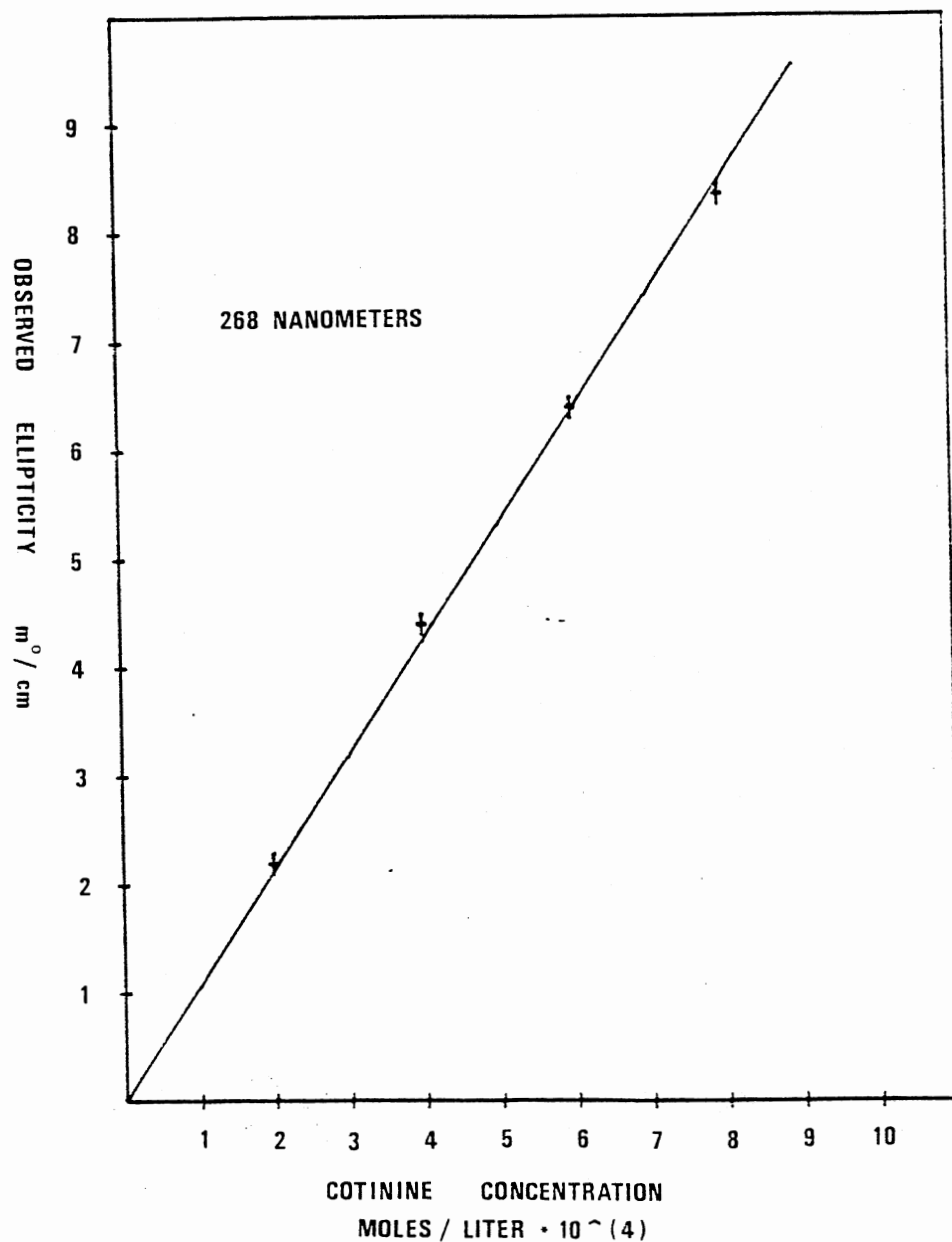
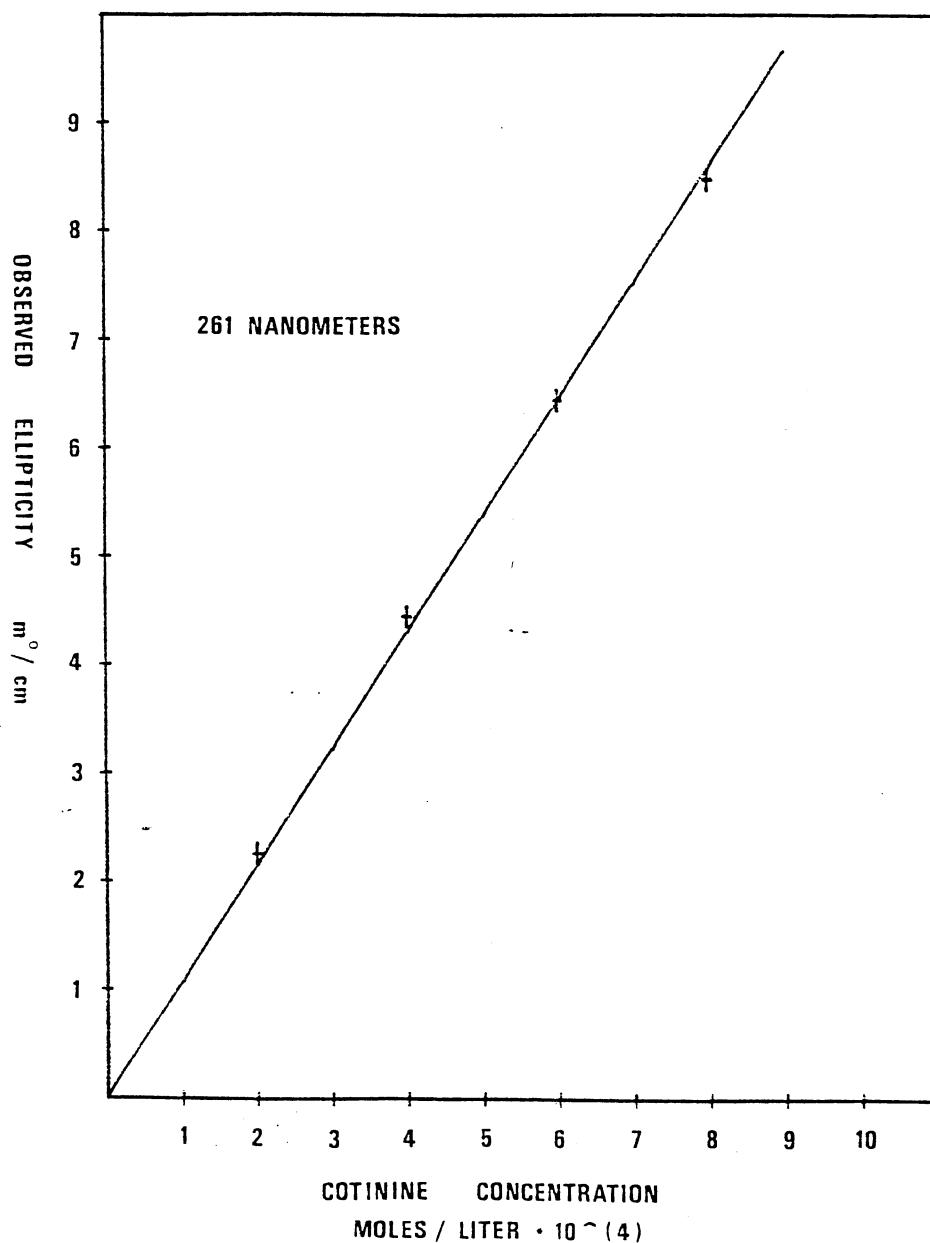


Figure 21. CD Spectra of Cotinine in 8.2 pH Buffer



Slope = θ = +10.62 Degrees Per Molar Solution Per Centimeter. Correlation Coefficient (r^2) = 0.999. Standard Deviation of the Slope = $8.99 \times 10^{-6}\%$. $M^{-1} \text{cm}^{-1}$.

Figure 22. Observed Ellipticity Versus Cotinine Concentration Calibration Curve and Linear Regression Analysis Statistics. Solvent: 8.2 pH Buffer



Slope = θ = +10.73 Degrees Per Molar Solution Per Centimeter. Correlation Coefficient (r^2) = 0.999. Standard Deviation of the Slope = $9.11 \times 10^{-6} \% M^{-1} cm^{-1}$.

Figure 23. Observed Ellipticity Versus Cotinine Concentration Calibration Curve and Linear Regression Analysis Statistics. Solvent: 8.2 pH Buffer

CHAPTER V

CONCLUSION

The successful application of CD to the determination of nicotine and its major metabolite, cotinine, demonstrate the future potential of the technique as a competitive approach for clinical determinations and quality control. The sensitivity and the selectivity of the method are consequences of the criteria required for CD activity. Sensitivity is comparable to that possible by UV absorption spectrophotometry, but selectivity is enhanced because two molecular requirements must be met before a compound is CD active. The freedom from any interferences that is gained because of these two requirements allows the exploitation of the method to produce unprecedented results within the domain of its usefulness. The future of the technique as a quantitative tool of analysis is conceivably very bright and provides the interested researcher an open realm of exploration.

The nicotine procedure outlined in this work could probably be developed to include other sample varieties such as the various types of leaf tobaccos, airborne nicotine residues, pesticides, and clinical extracts. The procedure could be used profitably in quality control determinations

in the tobacco industry.

The conclusions from the β CD complex studies compare well with the reported results from similar work on cocaine ($K_{\text{bind}} = 423$) and PCP ($K_{\text{bind}} = 1200$) (30). K_{bind} information alone provides little information on the complexation mechanism. All guests have an aromatic chromophore which presumably occupies the hydrophobic center of the sugar host, perhaps displacing the solvent. But the uncomplexed moiety of the guest must also be considered in the thermodynamics of the process. Further studies, in which the enthalpies and entropies of complexation are measured, are indicated whereby a better understanding of how these and other analogous complexes are formed between the body proteins and molecules that are foreign to the human body.

The cotinine results did not turn out to be as lucrative as was anticipated in the beginning. The fundamental interest of the cotinine study was to develop a method for the determination of binary nicotine/cotinine mixtures since the two often exist together. Determinations of binary mixtures of cocaine with a variety of other components have been successfully completed (31). In these cases, the components CD spectra were significantly different. In the nicotine/cotinine case, the spectra are too similar for a successful direct determination.

A SELECTED BIBLIOGRAPHY

1. Glover, E. D. and Henderson, A. H., Journal of Early Adolescence, 2(1), 1 (1982).
2. Merck Index 9th Edition, Merck and Co., Inc. Rathway New Jersey. Windholz, M. (Editor).
3. Clarke, E. G. C. "Isolation and Identification of Drugs", Vol. 1, William Glove and Sons Ltd., London, 1978.
4. Ferguson, B. B., Wilson, D. J., Schaffner, W., Amer. Journal of Dis. Child, 130, 837 (1976).
5. Haag, H. B. and Larson P. S., J. Pharmacol 78, 343 (1943).
6. McKinnis, H., Jr., Tobacco Alkaloids and Related Compounds, 4th Wenner-Gren Centre Int. Symposium, 4, Euler, U. S. von, (Editor), Oxford Pergamon, London, 1965.
7. Kaempe, B., Arch. Pharm. Chem., 81(21), 1183 (1974).
8. Watson, I. D., J. Chromatogr., 143(2), 203 (1977).
9. Rueker, G., Arch. Pharm., 310(6), 485 (1977).
10. Blass, K. G., Thihart, R. J. and Draisey, T. F., Journal Chromatogr., 95(1), 75 (1974).
11. Testa, B. and Jenner, P., Mol. Pharm., 9, 10 (1973).
12. Crone, T. A. and Purdie, N., Anal. Chem., 53, 17 (1981).
13. Peel, H. W. and Perrigo, B., J. Can. Soc. Forensic Sci., 9(2), 69 (1976).
14. Bowen, J. M and Purdie, N., Anal. Chem., 53, 2239 (1981).

15. Biot, J. B., Mem. Prem. Classe Inst. France, 13, 218 (1812).
16. Biot, J. B., Mem. Acad. Sci. Toulouse, 2, 41 (1817).
17. Lambert, J. B., Shurrall, H. F., Verbit, L., Cooks, R. G. and Stout, G. H., "Organic Structural Analysis", Macmillan, New York, 1972.
18. Abu Shumays, A. and Duffield, J. J., Anal. Chem., 38, 29A (1966).
19. Chan, R. S., Ingold, C. and Prelog, V., Angew. Chem. Inter. Edit., 5, 385 (1966).
20. Lach, J. L. and Pauli, W. A., J. Pharm. Sci., 55, 32 (1966).
21. Harata, K. and Uedaria, H., Bull. Chem Soc. Japan, 48(2), 375 (1975).
22. Cramer, F., Seanger, W. and Spataz, H. -Ch., J. Amer. Chem. Soc., 87, 2779 (1956).
23. DeMarco, P. V. and Thacker, A. L., Chem. Commun., 2 (1970).
24. Monk, C. B., "Electrolytic Dissociation", Academic Press, London, New York, 1961.
25. Pillsbury, H. C. and Bright, C. C., J. of the A.O.A.C., 55(3), 636 (1972).
26. Kaiser, H., Pure and Appl. Chem., 34, 35 (1973).
27. Weast, R. C., "CRC Handbook of Chemistry and Physics", 61 Edition, R. C. Weast (Editor), CRC Press Inc, Boca Raton, FL, 1981.
28. Pinner, Arch. Pharm., 231, 378 (1883).
29. Frankenburg, W. G. and Vaikekunas, A. A., Journal Amer. Chem. Soc., 79, 149 (1957).
30. Bowen, J. M., Atkinson, W. M., Crone, T. A. and Purdie, N. Unpublished results.
31. Atkinson, W. M., Bowen, J. M. and Purdie, N. Unpublished results.
32. Steel, R. G. D. and Torrie, T. H., "Principles and Procedures of Statistics. A Biometrical Approach", 2nd. Edition, McGraw-Hill, New York, 1980, p. 267.

APPENDIX

The algorithm for the linear regression analysis that was applied to the calibration curves was based on the linear model:

$$Y = bX$$

This treatment forces the y-intercept through the origin, a condition that is required by the theory used in the derivation of equation 2.5.

The slope is calculated by:

$$b = \frac{E(XY)}{E(X^2)}$$

The correlation coefficient (r^2) is calculated by:

$$r^2 = \frac{(E(XY))^2}{E(X^2) E(Y^2)}$$

A more descriptive study of the statistical analysis involved with this treatment can be found in the book by Steele and Torrie (32).

VITA

William Marc Atkinson

Candidate for the Degree of
Master of Science

Thesis: THE DIRECT DETERMINATION OF NICOTINE BY
CIRCULAR DICHROISM SPECTROPOLARIMETRY

Major Field: Chemistry

Biographical:

Personal Data: Born in Pine Bluff, Arkansas, August
21, 1958, the son of Mr. and Mrs. W. K. Atkinson
Pine Bluff, Arkansas.

Education: Graduated from Pine Bluff High School, Pine
Bluff, Arkansas May, 1976; recieved the Bachelor
of Science from Ouachita Baptist University,
Arkadelphia, Arkansas, August, 1980, with a major
in chemistry; completed the requirements for the
Master of Science degree at Oklahoma State Univer-
sity in May, 1983.

Professional Experience: Graduate Teaching Assistant,
Oklahoma State University, 1980-1983; Graduate
Research Assistant, Oklahoma State University,
1981-1983.

Professional Organizations: Phi Lambda Upsilon
Honorary Chemical Society, Blue Key Honorary
Fraternity.